AD-A145 820 DEFLOCCULANTS FOR TAPE CASTING BARIUM TITANATE(U) 1/1
RUTGERS - THE STATE UNIV NEW BRUNSWICK N J DEPT OF
CERAMICS W R CANNON JUL 83 TR-3 N00014-82-K-0313

UNCLASSIFIED F/G 13/8 NL

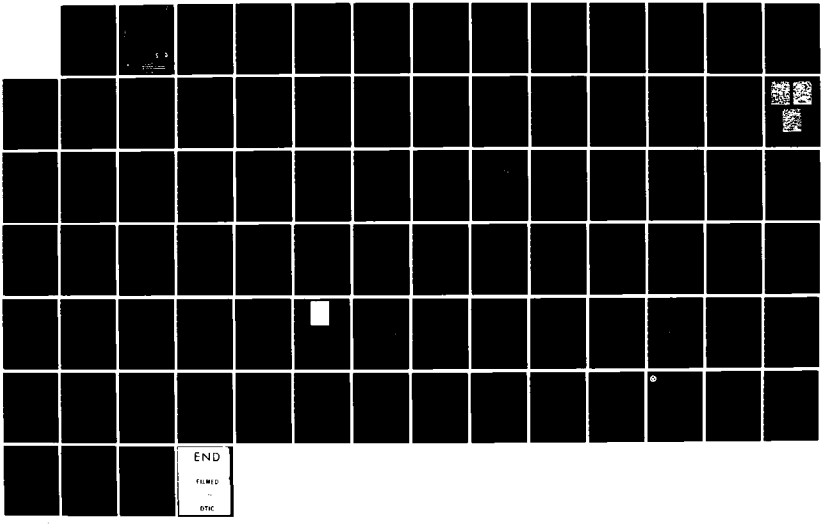

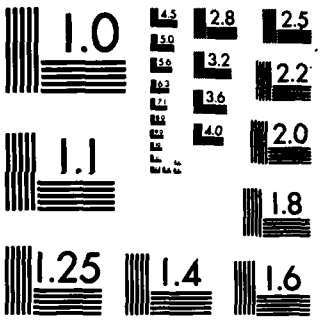

MICROCOPY RESOLUTION TEST CHART
NATIONAL BUREAU OF STANDARDS-1963-A

DEFLOCCULANTS FOR TAPE CASTING

BARIUM TITANATE

RUTGERS
THE STATE UNIVERSITY
OF NEW JERSEY
DEPARTMENT OF CERAMICS
COLLEGE OF ENGINEERING

Technical Report No. 3

Contract N00014-82-k-0313

DEFLOCCULANTS FOR TAPE CASTING

BARIUM TITANATE

W. R. Cannon
Department of Ceramics
Rutgers, The State University of New Jersey
P. O. Box 909
Piscataway, NJ 08854

July 1984

Annual Report for Period March 1983-March 1984

Prepared for the
Office of Naval Research
800 North Quincy Street
Arlington, Virginia 22217

REPORT DOCUMENTATION PAGE

READ INSTRUCTIONS BEFORE COMPLETING FORM

1. REPORT NUMBER: 3	2. GOVT ACCESSION NO.
3. RECIPIENT'S CATALOG NUMBER	
4. TITLE (and Subtitle): Deflocculants for Tape Casting Barium Titanate Dielectrics	5. TYPE OF REPORT & PERIOD COVERED: Annual Report March 1983-March 1984
6. PERFORMING ORG. REPORT NUMBER	
7. AUTHOR(s): W. Roger Cannon	8. CONTRACT OR GRANT NUMBER(s): N0014-82-k-0313
9. PERFORMING ORGANIZATION NAME AND ADDRESS: Department of Ceramics, Rutgers, The State University of New Jersey	10. PROGRAM ELEMENT, PROJECT, TASK AREA & WORK UNIT NUMBERS: NR651-008
11. CONTROLLING OFFICE NAME AND ADDRESS: Office of Naval Research, 800 North Quincy Street, Arlington, Virginia 22217	12. REPORT DATE: July 1983
	13. NUMBER OF PAGES
14. MONITORING AGENCY NAME & ADDRESS(if different from Controlling Office)	15. SECURITY CLASS. (of this report)
	15a. DECLASSIFICATION/DOWNGRADING SCHEDULE

16. DISTRIBUTION STATEMENT (of this Report)

Unlimited

17. DISTRIBUTION STATEMENT (of the abstract entered in Block 20, if different from Report)

Unlimited

18. SUPPLEMENTARY NOTES

19. KEY WORDS (Continue on reverse side if necessary and identify by block number)

Dielectrics, Barium Titanate, Deflocculants, Dispersants, Tape Casting

20. ABSTRACT (Continue on reverse side if necessary and identify by block number)

The dispersion properties of dispersants with barium titanate were studied. Rheological, settling volume and adsorption isotherms were obtained for barium titanate in MEK-ethanol using a phosphate ester dispersant.

Effects of storage conditions, dispersants and order of addition of tape casting components on the ultimate strength of green tapes was determined.

DD FORM 1 JAN 73 1473

Table of Contents

List of Figures

List of Figures (Continued)

Acknowledgement

The major portion of the research described in this report was performed by Mr. Kurt Mikeska in fulfillment of the research requirement for his Masters of Science Degree. Also contributing to this report was Mr. John R. Morris who is beginning his PhD studies. Undergraduate students who have contributed considerably to this report are Ms. Linda Braun and Ms. Susan Forti.

This research program is being performed in close cooperation with another Office of Naval Research sponsored program in the Rutgers Department of Ceramics entitled "A DLTS Study of Grain Boundaries in $BaTiO_3$ and Improved Particle Size Distribution of Tape Casting $BaTiO_3$" under the direction of Dr. John B. Blum.

Publications

1. Kurt R. Mikeska and W. Roger Cannon, "Dispersants for Tape Casting Pure Barium Titanate", to be published in Advances in Ceramics, Vol. 9, Forming of Ceramics, American Ceramic Society.

2. Kurt R. Mikeska and W. Roger Cannon, "The Dispersion of $BaTiO_3$ with a Phosphate Ester", to be submitted to the Journal of the American Ceramic Society.

3. Susan Forti, John R. Morris and W. Roger Cannon, The Green Strength of Cast Tapes", submitted to the Bull. of the American Ceramic Society.

4. Linda Braun, John R. Morris, and W. Roger Cannon, "Binder and Plasticizer Effects on the Viscosity of Tape Casting Slips" Submitted to the Bull. of the American Ceramic Society.

Presentations (this year)

1. K. Mikeska and W. R. Cannon, "Dispersants for Tape Casting Pure $BaTiO_3$, Electronic Division Meeting American Ceramic Society, Fall 1983.

2. Kurt R. Mikeska and W. R. Cannon, "Adsorption of Dispersants onto Barium Titanate", Presented at the Annual Meeting of the American Ceramic Society, May 1984.

3. Linda Braun, Susan Forti, John R. Morris, W. R. Cannon, "Strength of Cast Tapes of $BaTiO_3$ using Several Binder-Dispersant Combinations", Presented at the Annual Meeting of the American Ceramic Society, May 1984.

4. Kurt R. Mikeska and W. R. Cannon, "Dispersion of $BaTiO_3$ in the MEK-Ethanol System", Presented at the 58th Colloid and Surface Science Symposium, American Chemical Soc., Pittsburgh, June 1984.

I. Introduction

The overall goal of the research being performed under this contract is to improve the uniformity and density of tape-cast and sintered barium titanate dielectrics. The project specifically focuses on dispersants for use in nonaqueous tape casting systems.

A major concern of multilayer capacitor manufacturers is the reliability of the dielectrics. Although it is still not certain what roll voids in the dielectric have in decreasing the reliability, the likelihood is they have some roll and should be eliminated. Proper dispersion of the powder in the slip prior to tape casting is important in elimating voids. Most voids in the cast tape result from incomplete dispersion of the powder in the liquid vehicle and there is ample evidence that these interagglomerate voids are difficult to eliminate during sintering.

The approach we have taken in this research program is to screen a large number of commercial dispersants by rheological measurements and then to decide on two or more dispersants to study more thoroughly in an effort to understand what constitutes an effective dispersant and by what mechanisms they operate.

1.1 Achievements and Future Plans

a) During the second year of this contract we have accomplished most of the goals we had set to be completed by this time. Our achievements are:

First Year

1. Approximately 70 commercial dispersants were screened and the three best, a phosphate ester, an ethoxolate, and Menhaden Fish Oil were chosen for further studies.

2. Viscosity measurements and settling volume measurements were performed as a function of phosphate ester concentration.
3. Based on viscosity measurements and electrophoresis measurements a model was proposed for the dispersion effectiveness of the phosphate ester.

Second Year

1. The effects of water in the solvent and of aging of the suspension on the viscosity was measured.
2. The shear thinning and thixatropic behavior of the slips near the minimum viscosity was determined.
3. The rheological behavior of slips using fish oil as a dispersant was compared with the phosphate ester.
4. An adsorption isotherm for the phosphate ester was measured.
5. The model for phosphate ester was further developed including some estimates of the adsorption configuration and the free energy of adsorption.
6. Preliminary experiments showing the effects of order of addition of dispersant and binder were made.
7. The effects of aging conditions on the strength of the green tape was studied.

Some of the objectives of the originally proposed research which have not been acheived are:

1. The relationship between viscosity and adsorption isotherm for wet solvents and aged suspensions has not been completed. (There has been some difficulty in obtaining isotherms since

the phosphate ester adsorption peaks were not detectible in the IR spectra).

2. Infrared spectroscopy of the powder surfaces to determine the mechanism of attachment of dispersant to powder has not yet been completed.

3. The effect of binder and other organics on the effectiveness of the dispersant is only just beginning to be measured.

1.2 Future Plans

1. The phosphate ester dispersion mechanism has not been fully determined. The importance of electrostatic and steric hindrance will further be studied by adding to viscosity, settling volume and adsorption measurements, zeta potential vs. concentration of ester, solution pH and conductivity vs. concentration of ester. These experiments are in progress.

2. This study has proposed that the phosphate ester is held tightly to the particle via an ionic adsorption mechanism. The use of IR spectroscopy is probably the best method for characterizing interactions which occur at the solid/liquid interface, and it will be used to qualitatively substantiate the ionic mechanism. An FTIR with excellent detection capabilities is now available in the Department of Ceramics.

3. This study has demonstrated that water in the system strongly affects the dispersibility of the barium titanate powder. Thus, it is of interest to characterize the surface of the powder in terms of surface hydroxyls and strongly adsorbed molecular water. IR spectroscopy could be used to characterize the powder surface

water by measuring OH stretching bonds arising from specific types of adsorbed water.

4. The literature indicated that the nature of the liquid phase has an effect on adsorbate adsorption and dispersion effectiveness. Work is already underway to determine the effects of various solvents or mixtures of solvents on dispersion and adsorption.

5. The addition of binders and plasticizers to the system may affect adsorption of dispersants onto the barium titanate surface, and thus affect dispersibility. Additional work will be performed to determine the effects of binders and plasticizers on the dispersion of the powder and to examine more fully the effects of order of binder addition.

In order to carry out this research, John R. Morris, a PhD candidate, is being supported by this contract and in addition, Kurt Mikeska, is continuing the research reported in this annual report but is being supported by Rutgers University. Results from both students will be reported in the final report.

EXPERIMENTAL PROGRESS

II. EXPERIMENTAL PROCEDURE

2.1 Starting Materials

An initial objective of this research was to choose a standard system representative of a composition typically used by commerical manufacturers of tape cast multilayer capacitors. For simplicity, however, in the beginning suspensions contain only solvent, dispersant and powder were studied.

The following materials were selected in an effort to duplicate a non-aqueous system that could be utilized for commercial purposes.

The binder chosen to provide mechanical strength in the cast green tape was acryloid B-7 MEK 30 wt% solution supplied by Rohm and Haas Co. This is an acylic resin with low ash burn out supplied as a 30 wt% solution in methyl ethyl ketone (MEK).

The plasticizer used in the cast green tapes was Santicizer 160 supplied by Monsanto Inc. Santicizer 160 is a butyl benzyl pethalate used to provide green tape flexibility and reduce cracking in the dried tape.

HPB (high purity) barium titanate, lot 567, manufactured by Tam Ceramics Inc. was used as the dielectric throughout this study. Lot analysis as supplied by Tam Ceramics is indicated in Table I. Included in this table for comparison are BET* specific surface areas and density** measurements conducted during this study. This grade of barium titanate was manufactured by an oxalate co-precipitate process, calcined at 850°C, and subsequently spray dried (1).

The liquid used to disperse the barium titanate was an azeotrope mixture of methyl ethyl ketone and ethanol. An azeotrope of MEK-ethanol was chosen as the solvent because of its low inherent viscosity and low heat of vaporization. The azeotrope consisted of 66 wt% MEK and 34 wt% ethanol.

---

*Density measurements were conducted on a Micromeritics Instrument Corp. Autopycnometer 1320.

**Specific surface area was measured on a Quantachrome Corp. Quantaborb Sorption System.

Fisher Reagent grade MEK was used throughout this study. MEK has a molecular weight of 72.11, a density of .7996 g/cm^3 at 25°C, a viscosity of 0.20 cps at 25°C, and a chemical formula of $CH_3CH_2COCH_3$.

Fisher Reagent grade ethanol was used for all experiments except those conducted under dry conditions and those for argon plasma emission spectroscopy analyses. Ethanol used for these experiments was an absolute ethyl alcohol supplied by Florida Distilleries. Ethanol has a molecular weight of 46.07, a density of .80363 g/cm^3 at 25°C, a viscosity of 1.2 cps at 25°C, and a chemical formula C_2H_5OH.

Table I - Lot Analyses for HPB (lot 567) Barium Titanate Powder

Loss on Ignition (TAM)	0.33%
+325 Mesh (TAM)	<.01%
B.E.T. specific surface (TAM)	3.56 m^2/g
B.E.T. specific surface (this study)	3.5 m^2/g
Density (TAM)	5.5 g/cm^3
Density (this study)	5.9 g/cm^3
BaO/TiO_2 mole ratio (TAM)	0.997
Fisher number (TAM)	1.19

2.1 Moisture Content: Karl Fischer Reagent Method

It was of interest to determine the moisture content of the individual components of our system in order to determine the effects of water on dispersion properties. The Karl Fischer reagent method (KFR) was used for determining free water and bound water (water of hydration). Procedures for measurement of water were followed according to ASTM. E203-64 and are discussed in detail by Mitchell and Smith (2). The measurement of free and bound water was performed by titration to an electrometric end point by the dead-stop (biamperometric) technique using a Fisher Model 391 aquametry apparatus. The fundamental theory behind this technique is reviewed in the literature (2). Karl Fischer reagent was used as a titrant and was standardized using a standard water-in-methanol solution. For the analysis of water in soluble and insoluble materials, it is convenient to use dry methanol as a solvent for dilution of the samples. However, a stoichiometric interference was created with the determination of free water in our methyl ethyl ketone solvent, therefore, pyridine, instead of methanol, was used as a standard solvent for all substances tested.

Calculation of the water content of soluble liquids was as follows:

$$\text{percent water} = [(AF \times 0.001)/W] \times 100, \qquad (2.1)$$

where A is ml of KF reagent required for tetration, F is the water equivalent in mg of water per ml of KF reagent, and W is grams of sample. Titrations were performed at 25 ± 1°C.

For insoluble materials, such as the barium titanate powder, the solid was added to the pyridine solvent and magnetically stirred for one hour at room temperature and allowed to settle. An aliquot of the supernatent was withdrawn and titrated. Calculations of the water content of insoluble solids was as follows:

$$\text{percent water} = [((A-B)F \times .001)/W] \times 100, \qquad (2.2)$$

where A, F, and W are as previously mentioned, and B is the number of ml of KF reagent required to titrate a solvent blank. Results are found in Table II.

Table II. Water Contents as Determined by Karl Fischer Methods

	Ambient (%)	(Dry) %
Methyl Ethyl Ketone	0.0338	0.0068*
Ethanol	5.1029	0.0161*
MEK-ethanol	1.8658	0.0059*
Barium Titanate Powder	0.1229	0.1120**

*Solvent was dried over Linde molecular sieve.
**Powder was vacuum dried at 300°C.

2.3 Assessment of Dispersibility of Phosphate Ester

A phosphate ester* was found to be an effective dispersant. Viscosity as a function of dispersant concentration was employed to determine the optimum point of dispersion of the phosphate ester under ambient, dry, and aged conditions.

*Emphos PS-21A, Witco Chemical Co.

For each condition, a series of dispersion samples of each concentration of phosphate ester were prepared. Concentrations ranged from 0.2 vol % to 2.0 vol % phosphate ester. Dispersion samples were analyzed at 50 vol % solids suspended in the MEK-ethanol azeotrope. Sample size was 16.36 ml. Samples were agitated ultrasonically for 2.0 minutes at 40 W/cm^2 and cooled in an ice batch during sonification. A 2X HAT Brookfield** cone-plate microviscometer was used to make apparent viscosity readings. The geometry of the cone-plate viscometer makes it a fundamental instrument. Each sample was subjected to the full range of its shear rates in order to determine slip rheology. The slip viscosity was taken immediately after agitation without regard to any thickening which might occur with time. The phosphate ester was used as received in all experiments. The as received Emphos PS-21A contained pure phosphate ester, i.e., the material had not been diluted or dissolved into solution. Measurements were taken at $25^{0}C \pm .5^{0}C$.

The dispersibility of powder using the phosphate ester was first assessed under ambient conditions. HPB barium titanate and Fisher reagent grade MEK-ethanol were used as received. Moisture content of each component is given in Table II.

The dispersibility of powder using the phosphate ester was then assessed after aging for a period of time. HPB barium titanate and Fisher reagent grade MEK-ethanol were used as received. Each sample was ultrasonicated for one minute, allowed to stand statically for

**Brookfield Engineering Laboratories, Inc.

twenty-four hours, and sonicated again for one minute. The slip viscosity was measured immediately after the second one-minute sonification treatment.

The dispersibility of powder using the phosphate ester was finally assessed under dry conditions. The solvents were dried statically over Linde* molecular sieves M.S. type 3A (1/6" pellets) prior to use in the dispersibility experiment. The molecular sieves were dried at 200°C for 24 hours in a circulating air oven before use. The sieve loading was 5:1 (g M.S./g solvent). The solvents were left in contact with the sieves for 24 hours. After drying over the sieve, the solvent was filtered with common filter paper into a clean, dry glass jar prior to use. Residual moisture, as determined by Karl Fischer reagent methods, is indicated in Table II. The Fisher reagent grade ethanol could not be dried sufficiently after treatment with the moecular sieves (residual moisture = 2.68% ± 0.02 mg), therefore, an absolute ethanol from Florida Distilleries was used and treated as indicated above.

The HPB barium titanate powder was dried at 300°C in a vacuum drying oven for 24 hours prior to use. The powder was allowed to cool at room temperature inside a dessicator containing calcium sulfate dessicant before use. Residual moisture, as determined by Karl Fisher reagent methods, is indicated in Table II.

*Alfa Products Corp.

2.3.1 Equilibrium Sedimentation Volumes

Centrifugal powder compacts were used to evaluate dispersibility and determine equilibrium sedimentation volumes of the phosphate ester dispersions. Samples were prepared in a manner identical to those used for the ambient phosphate ester experiment. All samples were centrifuged for 100 minutes at 2000 rpm in 25 ml polyethylene centrifuge tubes. Observations concerning the relative sediment heights were then recorded.

2.4 Electrophoretic Mobility

An electrophoresis test was performed to determine the nature of the surface charge on barium titanate particles suspended in both water and MEK-ethanol medias containing various surface active agents. Two platinum electrodes were inserted in dilute suspensions and a potential applied (12 V). Electrophoretic mobility was qualitatively determined by noting the quantity of deposition of particles on either the cathode or anode.

2.5 Adsorption Isotherms

Adsorption isotherms were plotted in order to determine the surface excess concentration of the phosphate ester dispersant adsorbed onto a unit area of barium titanate. To determine the change in solution concentrations that occurs on adsorption, known weights of the powder and liquid were brought together and allowed to come to equilibrium at a constant temperature. The resulting supernatent was then analyzed for residual solute.

Samples were prepared by mixing 61.875 g of barium titanate with 26.997 g of the MEK-ethanol-phosphate ester liquid which corresponds to 25 vol % solids. The concentration of the phosphate

ester was varied in each sample to correspond with the various concentrations of phosphate ester used in the rheology and settling experiment which were conducted at 50 vol % solids.

To establish equilibrium, the samples were mixed in a tumbling end over end type fashion in tightly sealed 50 ml polyethylene centrifuge tubes at 25°C ± 5°C for twenty-four hours. To allow for a more effective washing of the solid particles by the liquid solution, a 25 vol % solids concentration was used in this experiment instead of the 50 vol % solids concentration previously used in the rheology and settling experiments. A 50 vol % solids concentration dispersion is too viscous and inhibits the proper mixing action necessary to establish an equilibrium condition.

After equilibrium was established, the dispersion was centrifuged at 2000 rpms for 100 minutes. A 10 ml sample of the resulting supernatent was withdrawn by a syringe for analysis.

The supernatent was analyzed to determine the equilibrium concentration of phosphate ester remaining in the solution by a commercial analytical laboratory* using argon plasma emission spectroscopy. The supernatent was analyzed for phosphorous with a precision of ± 5 g/ml of solution. Since the number of molecules of phosphate ester are proportional to the number of atoms of phosphorous, grams of phosphorous can be converted to moles of phosphate ester by

$$\frac{Ng}{MWp}$$

where Ng is the number of grams of phosphorous per sample and MWp is the molecular weight of phosphorous.

A number of alternative quantitative characterization methods were considered for determining the equilibrium concentration of the phosphate ester in the supernatant without much success. Since the phosphate ester is a relatively strong acid, potentiometric non-aqueous titration of the acid by a base was considered feasible. However, the equilibrium concentration of the acid proved to be too dilute to allow for accurate and meaningful results.

Infrared spectroscopy was also considered. The P=O stretching vibration adsorption band occurring characteristically around 1200 cm^{-1} is ideal for identifying the phosphate ester, however, the adsorption band due to C-O stretching vibrations of the solvent occurring between 1200-1000 cm^{-1} makes quantitative analyses for the phosphate ester by infrared adsorption difficult.

Measurement by gas chromatography was considered on the basis that the retention time for the phosphate ester would be much greater than those for the MEK-ethanol solvent due to the phosphate ester's high molecular weight. Retention times proved to be extremely long due to the very high boiling point (735°C) of the phosphate ester and peak resolution was poor, thereby causing analyses by GC to be impractical.

2.5 Tape Composition, Casting, and Firing

To assess the effectiveness and compatability of the phosphate ester in the casting of actual tapes, slips utilizing the phosphate

*Luvak Inc., Boylston, MA.

ester were subsequently cast and fired. The composition of the casting slip was as follows: 45.0 vol % HPB $BaTiO_3$, 18.0 vol % acryloid B-7, 25.0 vol % MEK-ethanol, 5.0 vol % Carbowax*, 5.0 vol % Santicizer 150, 1.0 vol % Cyclohexanol, and 0.75 vol % Emphos PS-21A.

Batches were prepared using 50.0 g of $BaTiO_3$. First the MEK-ethanol, Santicizer, Carbowax, Cyclohexanone, and Emphos were mixed with a stirring rod in a glass beaker. The $BaTiO_3$ was then added slowly while continuously stirring. After all the powder has been added, the slip was sonicated for three minutes at 40 W/cm^2. The acryloid was then added, and the entire slip was stirred with a stirring rod. The slip was next magnetically mixed for thirty minutes. The beaker was sealed during mixing to prevent solvent evaporation. After magnetic mixing, the slip was filtered by passing it through a nylon filter situated in the bottom of a large syringe. Before casting, the slip was deaired in a vacuum for 5 minutes.

Casting was performed on a bench scale caster**. Casting head speed was 0.36 ft/min. After drying in an ambient atmosphere, the green tapes were stripped from the substrate and stored in a dessicator.

The firing of the green tapes to sintered compacts was done in a C and M Inc. rapid temperature furnace in air. The green tapes were first fired to 500°C over an eight hour period to burn out binders and plasticizers. The tapes were cooled to room temperature

*Carbowax 400, Fisher Scientific Co.

**Model 133A, Claden, Inc.

before final firing. Firing to a sintered compact was achieved by heating at a rate of 3°C/min to 1400°C with a one-hour soak at final temperature and subsequently cooling at the same 3°C/min rate. Fired tapes were stored in a dessicator.

III. RESULTS AND DISCUSSION

3.1 Screening Tests

As described in a previous report[3], approximately 70 commercial dispersants were evaluated for compatability with the MEK-ethanol azeotrope by a solubility screening test. Twenty-nine of those dispersants determined to be soluble were further tested by a rheological screening test. The three most effective dispersants, in order of their effective dispersibility, were found to be a phosphate ester*, a fatty acid**, and an ethoxylate***.

3.2 Assessment of Dispersibility of Phosphate Ester

From the screening of the various commercial dispersants, it was determined that using the phosphate ester the viscosity decreased most rapidly with concentration. Thus the dispersion properties of the phosphate ester were further studied by rheological and settling methods. Since absolute viscosity values were desired, viscosity measurements were performed with a Brookfield coneplate viscometer.

---

*Emphos PS-21A, Witco Chemical Co.

**Menhaden Fish Oil, Spencer Kellogg Co.

***Zonyl A, E. I. du Pont de Nemours & Co.

Preliminary viscosity measurements indicated the phosphate ester was sufficiently effective to allow rheological measurements to be made at a very high volume fraction of solids (50 vol % solids). It should be noted that concentrated suspensions behave differently than dilute suspensions due to an increase in the volume of the dispersed phase and a decrease in the volume of the continuous phase, resulting in closer interparticle spacing and increased interparticle interactions on application of shear.

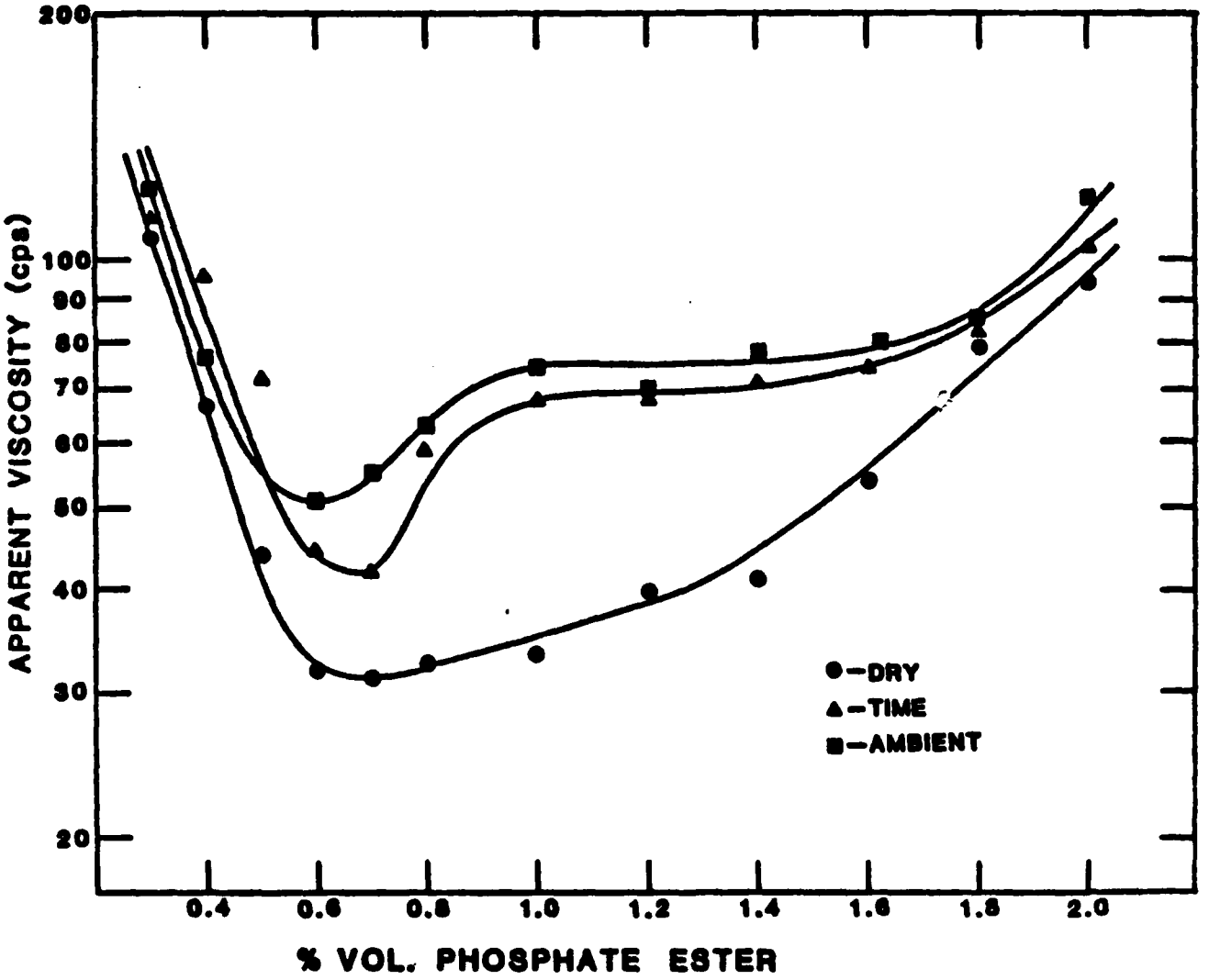

Figure 1. Apparent viscosity as a function of phosphate ester concentration for dry, aged, and ambient dispersions.

Figure 1 shows measured apparent viscosity as a function of phosphate ester concentration under ambient, dry, and aged conditions. Water content of each component, as indicated by Karl Fischer methods, is shown in Table II. The ambient MEK-ethanol azeotrope had a total water content of 1.865%, and the ambient barium titanate powder had a total water content of 0.123%. The MEK-ethanol azeotrope dried over molecular sieve had a total water content of just 0.0059%, and the vacuum dried powder had a water content of 0.1120%. These results indicate that the dry materials contained substantially less water than the ambient materials. Time considerations were measured only under ambient conditions. A minimum viscosity of 51 cps was measured under ambient conditions at 0.6 vol % phosphate ester. The dispersions that were allowed to age for twenty-four hours had a minimum viscosity of 42 cps at 0.7 vol % phosphate ester, and the dry dispersions had a minimum viscosity of 29 cps at 0.7 vol % phosphate ester. The maximum degree of dispersion for each of the conditions tested occurred at approximately 0.7 vol %. At concentrations less than 0.7 vol %, viscosity increased as the dispersions became more underdeflocculated, and at concentrations greater than 0.7 vol %, viscosity increased as the dispersions became increasingly overdeflocculated.

SEM micrographs, as seen in Figure 2, were taken of powder compacts at the point of maximum dispersion, at underdeflocculation, and at overdeflocculated. The micrographs indicate, on a qualitative basis, that the underdeflocculated cast (0.2 vol %) and overdeflocculated cast (1.9 vol %) had a much greater degree of agglomeration than the cast material examined at the point of maximum deflocculation (0.7 vol %).

0.2% PHOSPHATE ESTER

1.9% PHOSPHATE ESTER

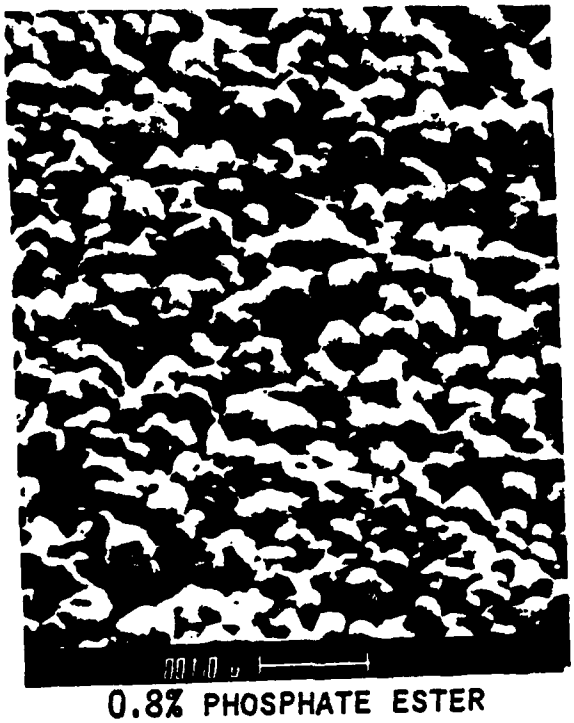

0.8% PHOSPHATE ESTER

Figure 2. SEM micrographs of the top surface of the centrifuged cake at underflocculation (0.2 vol %), at overflocculation (1.9 vol %), and at the point of maximum dispersion (0.8 vol %).

On the basis of viscosity, the order of increasing dispersion for the dry, time, and ambient disperison is as follows: dry > time > ambient. These results indicate a definite effect on dispersion due to moisture and time.

Comparing the viscosity curves of the ambient dispersions and the dry dispersions, there is a general increase in viscosity of the ambient over the dry. Considering the effects of water, Tormey (4) has shown by IR adsorbance at the solid/liquid interface in alumina/fish oil/toluene that adsorption bands between 3480 cm^{-1} and 3100 cm^{-1} are attributed to surface hydroxyls and adsorbed molecular water. When comparing the interface under ambient (air dried powder) and dry (vacuum dried powder), a large drop in intensities between 3480 cm^{-1} and 3100 cm^{-1} was observed due to removal of molecular water. She also observed a slight enhancement in dispersant adsorption under dry versus ambient conditions. The IR spectra of just an air dried alumina indicated an intense band at 3480 cm^{-1} -3407 cm^{-1} and can perhaps be correlated with the presence of adsorbed molecular water. She concluded that even when vacuum dried, there is at least a monolayer of undissociated water molecules that are hydrogen bonded to surface hydroxyls. Tormey's results indicate that removal of molecular water is difficult and can affect adsorption of dispersants.

In the case of the barium titanate system, it was calculated that 2.8×10^{19} molecules of water per gram of barium titanate represents a monolayer of water covering the particle surface using a value of 0.125 nm^2 as the area of a water molecule. According to Karl Fischer results, the vacuum dried powder contained 0.112% of water which corresponds to 3.57×10^{19} molecules of H_2O per gram of

barium titanate. This value is very close to the value for a monolayer of coverage. The ambient powder contained 4.11×10^{19} molecules of water per gram of barium titanate. Both conditions indicate that there is at least a monolayer of molecular water adsorbed onto the particle surface. Vacuum drying at 300°C does little to further remove this strongly adsorbed layer of water, let alone remove surface hydroxyls. The addition of the liquid components can only add to this already adsorbed layer, especially under ambient conditions, where it was shown that a substantial amount of water was present in the liquid phase.

Since viscosity is an indication of the degree of dispersion and particle agglomeration, where the ambient dispersions had a higher apparent viscosity than the dry dispersion, the ambient suspension was apparently dispersed to a lesser extent than the dry suspension due to molecular water present in the liquid phase and molecular water adsorbed onto the barium titanate surface. There is also a possibility that water present in the bulk solution is co-adsorbed along with the dispersant causing a reduction in repulsive potential energy forces between particles. This will be discussed further in Section 3.7.

A comparison of the viscosity curves of the aged (24 hours) dispersions and the unaged ambient dispersions indicated a general decrease in viscosity with time. It can be suggested that the amount of adsorbate adsorbed onto the barium titanate surface increases with time resulting in increased suspension stability. There are several factors which can influence the rate of adsorption of macromolecules from solution. These include the chemical nature of the adsorbate, adsorbate molecular weight, nature of the solvent,

and nature of the adosrbent (5). Adsorbent surface characteristics are perhaps the most important factor influencing adsorption equilibrium. Adsorption onto porous surfaces is usually slower than onto nonporous surfaces. Adsorption equilibrium on nonporous surfaces can occur within a few minutes while equilibrium on porous surfaces may take several hours to several days. The size of the surface pores in relation to the size of the the adsorbate molecules in the solution is also an important factor. There is also some evidence that adsorption equilibrium is directly related to the intrinsic viscosity of the liquid phase, where complete adsorption was proportional to the square of the intrinsic viscosity. It has also been shown that adsorption time is related to the molecular weight of the adsorbate, where equilibrium time increases with increasing molecular weight of the polymer due to the slow diffusion of large molecules into adsorbent pores. Adsorption may also be affected by the rate of diffusion of macromolecules into pores between hard agglomerates.

Scanning electron micrographs of the as received barium titanate powder indicated substantial agglomeration of small particles and some individual particle surface roughness, although resolution was not sufficient to reveal surface porosity; nevertheless, some surface microporosity can be assumed.

The resultant time effect can probably be partially attributed to the rate of diffusion of the phosphate ester into surface pores and interagglomerate pores, resulting in increased macromolecule adsorption with time and thus better dispersion. The phosphate ester also has a relatively high molecular weight which could prolong the time necessary to establish an equilibrium condition (5).

The time effect may also be influenced by the chemical nature of the MEK-ethanol solvent and the presence of molecular water adsorbed onto the adsorbent surface. There is a possibility that initially adsorbed water and solvent are replaced by the phosphate ester with time leading to increased dispersibility.

Regardless of the possible mechanisms that affects the stability of the barium titanate dispersion, we can conclude that there was a definite dispersion-time relationship.

3.3 Equilibrium Sediment Volumes

Equilibrium sediment volumes were used as a qualitative method to predict flocculation on the basis that dispersed systems give a more close packed structure while flocculated dispersions possess open interparticle networks due to agglomeration and thus higher sediment volumes (6,7).

Equilibrium volumes achieved by gravitational forces may not be reached for days or even weeks. Therefore, samples were centrifuged to a powder cake by low speed centrifugation. The forces experienced at low speed centrifugation do not usually alter the sediment volumes of a flocculated dispersion appreciably, as can high speed centrifugation, where large stresses can break the structure of weakly flocculated particles (6,7).

From equilibrium settling volumes, the volume fraction of packing, V_F, was calculated according to the following equation:

$$V_F = \frac{X_o V_o}{V_l}$$

where v_o is the initial suspension volume, V_1 is the ultimate sediment volume, and X_o is the initial volume fraction of solids. Packing fractions can be used to stimulate casting density and uniformity.

Equilibrium packing fractions as a function of the concentration of the phosphate ester are seen in Figure 3. A maximum packing fraction of 0.632 occurred between the concentrations 0.7 vol % and 1.0 vol % phosphate ester. These concentrations of phosphate ester corresponds quite well with the concentrations of phosphate ester at which minimum viscosity occurred. This appears reasonable since the point of minimum viscosity and the point of maximum sedimentation both correspond to minimum agglomeration and maximum dispersion. A packing fraction of 0.632 is quite good considering the fineness and narrow size distribution of the powder.

Scanning electron micrographs, as seen in Figure 2 and as previously discussed of the cast surfaces indicate that the most uniform and least agglomeration occurs at approximately 0.7 vol % phosphate ester.

The Quemada (8) equations has been used (9) in relating packing factors (γ_M) to relative viscosity η_r at high shear rates in the hydrodynamic range:

$$\eta_r = (1 - \phi/\phi_M)^{-2}, \qquad (3.1)$$

where ϕ is the volume fraction of solids in suspension and ϕ_M is the solid packed volume fraction. Figure 4 is a graphical representation of the equation for various volume fractions and packing fac-

tors plotting $_r$ against . By knowing the packing fraction and volume fraction of solids, it is possible to predict the relative viscosity of a dispersion.

A maximum packing fraction of 0.632 (Figures 5.6) was measured using the phosphate ester as a dispersant at 50 vol % solids. Using the Quemada equation, a relative viscosity of 23 is predicted for a fully dispersed system having hydrodynamic flow characteristics and a packing factor of 0.632. This value is fairly close to a relative viscosity of 36* calculated from the minimum viscosity measurement taken at 0.7 vol % phosphate ester under dry conditions. It is doubtful that a hydrodynamic flow condition was reached when viscosity measurements were taken in the phosphate ester systems. Therefore, the relative viscosities calculated for the phosphate ester suspension may actually be even closer to the value predicted by the Quemada equation.

3.4 Rheological Considerations

For practical considerations in tape casting it is important to consider the relationships between shear stress, shear rate, and history dependence.

---

*The relative viscosity was calculated using a viscosity of 0.8 cps for the continuous phase.

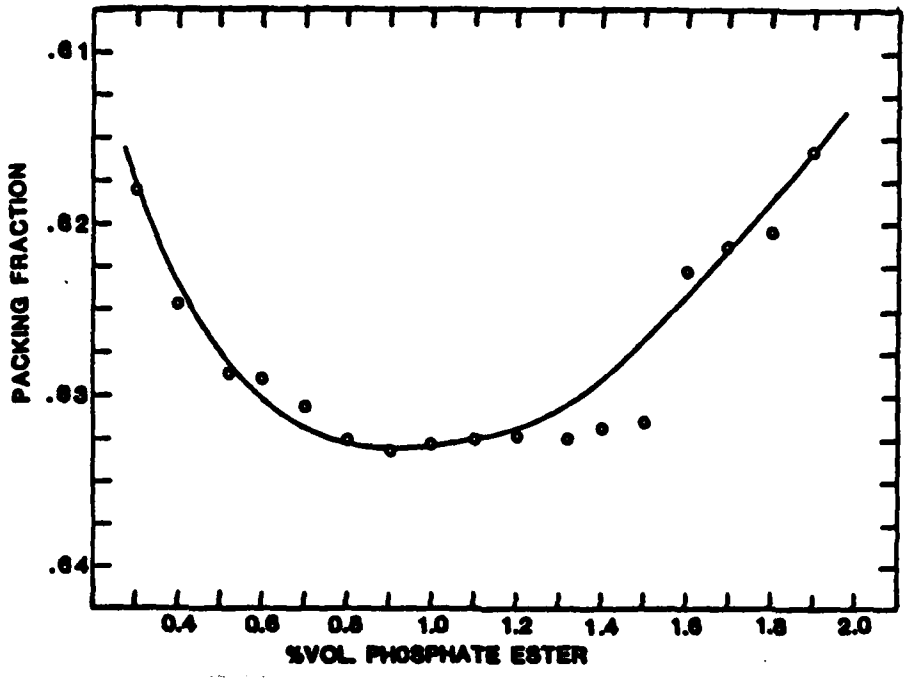

Figure 3. Packing fraction (% theoretical density) as a function of phosphate ester concentration.

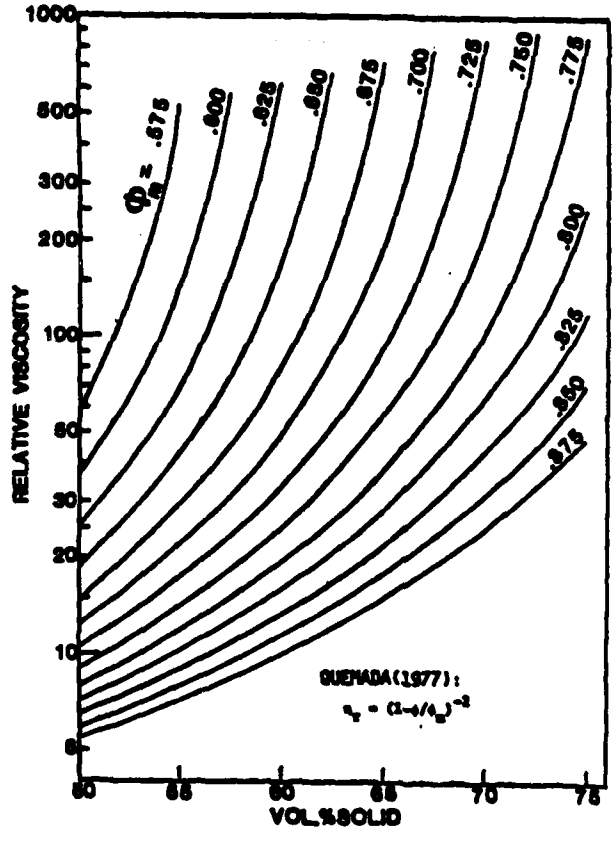

Figure 4. Graphical representation of Quemada's equation .

In order to determine the slip rheology, each sample was subjected to shear rates ranging from 3.84 sec^{-1} to 384 sec^{-1}. Samples were first measured at the lowest shear rates and then measured at continuously increasing rates until the highest rate was achieved. This procedure was then carried out in reverse order working from the highest rate to the lowest. This procedure provided an effective method for determining time dependency and stress behavior.

It was found that all dispersions, as a function of phosphate ester concentration, were shear thinning and thixotropic. The degrees of thixotropy and shear thinning varied considerably with phosphate ester concentration. On the basis of minimum viscosity, we have concluded that the degree of dispersion varies with the concentration of phosphate ester. Therefore, variations in shear thinning and thixotropy can be attributed to the degree to which each sample is dispersed as a function of phosphate ester concentration. It is also important to realize that these dispersions were highly concentrated (50 vol % solids). Highly concentrated dispersions react much differently to applied force than dilute suspensions due to increased interparticle contact.

Figure 5 indicates the degree of shear thinning as a function of phosphate ester concentrations for the ambient dispersions. As the concentration of phosphate ester is increased beyond the point of maximum dispersion (0.7 vol %), the dispersions became increasingly shear thinning as seen in the figure. The dispersions also became increasingly shear thinning as the concentration of phosphate ester was decreased below the point of maximum dispersion.

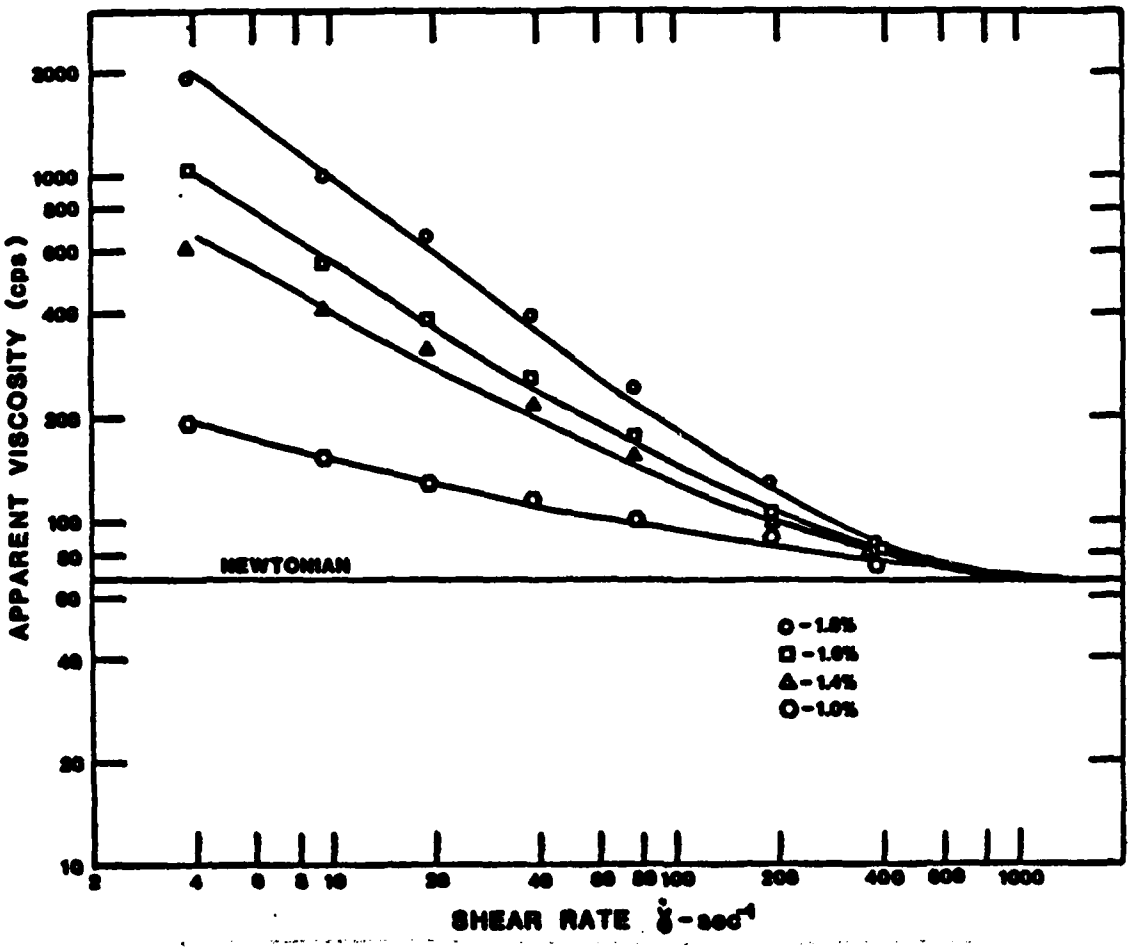

Figure 5. Viscosity-shear rate relation for varying concentrations of phosphate ester.

At the point of maximum dispersion, the suspendions act more Newtonian than the under and overflocculated systems.

Flocculated systems are known to have internal structures due to agglomeration. These structures are broken down with increasing shear forces. At under and overflocculated conditions, where agglomeration is prevalent, viscosity at low shear rates is very high as seen in the figure. As shear rate is increased, viscosity decreases as interal structure is broken down until Newtonian behavior is reached at high shear rates. At the point of maximum dispersion, (0.7 vol %) the degree of viscosity change as a function of shear rate is not as drastic indicating there is less of an internal structure.

From the results and the above discussion, it becomes evident that it is important to examine a dispersion over a complete range of shear rates in order to determine the degree of flocculation. At high shear rates dispersions act Newtonian, i.e., internal structure is broken down, and therefore dispersions with differing degrees of flocculation may have viscosity values that appear equal at high rates of shear, but at low shear rates there may be large differences in viscosities. Referring again to Figure 5 for the ambient dispersions, viscosities for concentrations of 1.0, 1.2, 1.6, and 1.8 vol % phosphate ester all have a viscosity of approximately 70 cps at high shear rates (384 sec^{-1}). Over a continuous range of shear rates, viscosities of the more flocculated dispersions were much higher than the more dispersed suspensions. In summary, shear thinning and thus interparticle structure increases as flocculation increases on either side of the point of maximum dispersion for the phosphate ester systems.

All dispersions showed some degree of shear thinning time dependency. Figure 6 for 1.0 vol % phosphate ester under ambient conditions is a typical example. Thixotropy is indicated by the characteristic hysteresis loop.

Time dependency is conveniently determined by measuring the viscosity of a slip at two points in time at identical rates of shear (384 sec^{-1}). Measurements were made by first subjecting the slip to a continuous range of shear rates starting at 3.84 sec^{-1} and continuing up to 384 sec^{-1}. The initial time, t_o, was the time at which the shear rate reached 384 sec^{-1} and then the viscosity, η_o, was measured. At this point the internal structure of the slip should be broken down by the high shear forces. The rate of shear

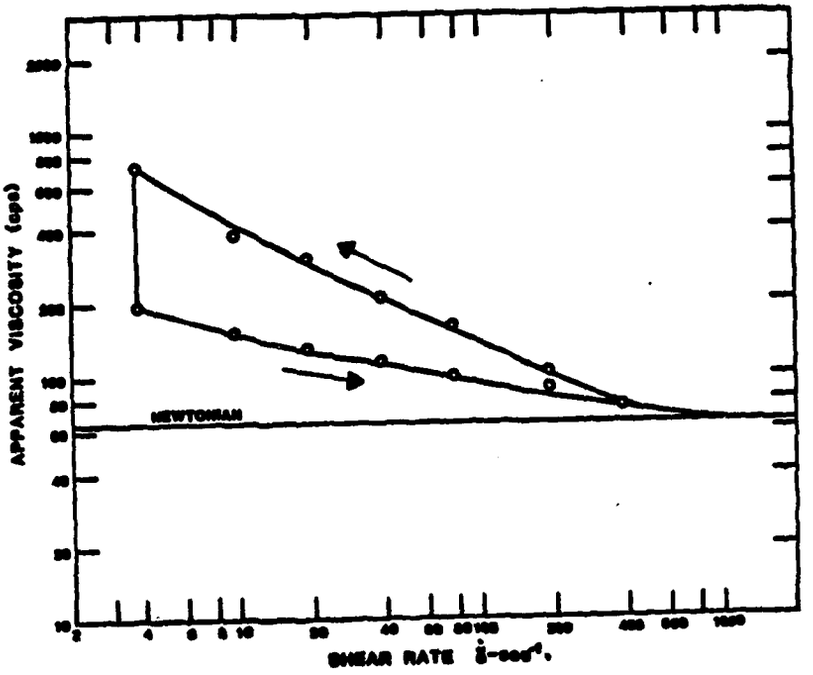

Figure 6. Diagram illustrating shear-thinning time dependency.

was then continuously decreased to 3.84 sec^{-1}. The slip has now had some time to relax and reform an internal structure. At this point the shear rate was returned directly to 384 sec^{-1}, and viscosity η_1 was measured. The difference between t_1 and t_o measures a degree of recovery of the system to its original structure and is a useful means of measuring thixotropy. The differences between η_1 and η_o are listed in Table III for the dry dispersions. These values indicate that as the dispersions became more flocculated on either side of the point of maximum dispersion the degree of thixotropy increases. Fully dispersed suspensions had almost monotonic behavior. Both the ambient and aged dispersions showed similar behavior.

It is known that flocculated systems have more of an internal structure than fully dispersed systems, and that dispersed systems have greater interparticle repulsion forces which reduce floccula-

tion and create stability. This suggests that when a system's internal structure is broken down by shear forces, fully dispersed systems will recover slower than flocculated systems due to repulsive forces, and if they do recover, the internal structure will be less agglomerated than those for flocculated systems. Thus, fully dispersed systems will be less thixotropic than flocculated systems. This is evident in the values seen in Table III. This also reinforces the hypothesis that maximum dispersion occurs at approximately 0.7 vol % phosphate ester.

3.5 Adsorption Model

To better understand the mechanism by which the phosphate ester stabilizes the barium titanate dispersion, a model for adsorption of the phosphate ester at the barium titanate/liquid interface was developed. The model takes into consideration dispersion forces and electron acceptor-donor interactions at the solid/liquid interface.

Phosphate esters are the esters of their corresponding oxyacids. Emphos PS-21A is the corresponding ester of phosphoric acid (10), as indicated in Figure 7. Phosphoric acid is tribasic in which one, two, or three of the acidic hydrogens of the hydroxyl groups are replaced by alkoxy groups. Emphos PS-21A is an equal combination of both mono-and dialkyl phosphate esters with a molecular weight of 525 to 530 for the monoalkyl ester and 950 for the dialkyl ester (10). The alkoxy function groups, as estimated from the corresponding molecular weight, are linear chains of about thirty carbons. The chains are unsaturated (11).

Table III. Viscosities (cps) Measured at t_o and t_1 for Dispersions

Concentration Phosphate Ester (vol %)	t_o	t_1	$t_1 - t_o$
0.4	66.0	73.6	7.6
0.6	32.0	34.56	2.56
0.7*	31.23	32	0.77
0.8	32.64	34.33	1.69
1.0	33.25	35.2	1.95
1.2	39.94	42.24	2.3
1.4	40.96	43.52	2.56
1.6	53.76	58.88	5.12
1.8	78.72	84.48	5.76
2.0	93.44	101.12	7.68

*Point of maximum dispersion.

The hydrogen of the hydroxyl groups of the mono- and dialkyl esters are highly acidic and readily dissociate in aqueous media to form anionic polyelectrolytes, as seen in Figure 8. Confirmation of proton dissociation was confirmed by a substantial drop in pH in both aqueous and non-aqueous (MEK-ethanol) medias on addition of the phosphate ester. Dissociation can be represented by a Lewis acid-base reaction.

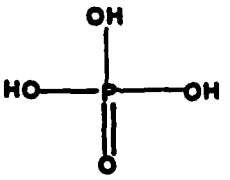

PHOSPHORIC ACID

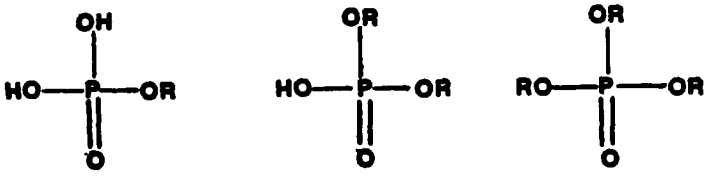

PHOSPHATE ESTERS

Figure 7. Phosphoric acid and its corresponding phosphate esters.

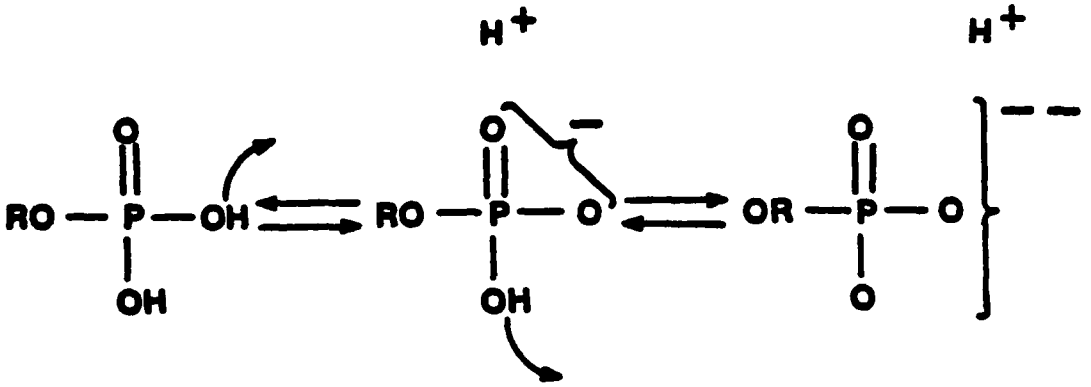

MONOANION DIANION

Figure 8. Ionization of phosphate esters.

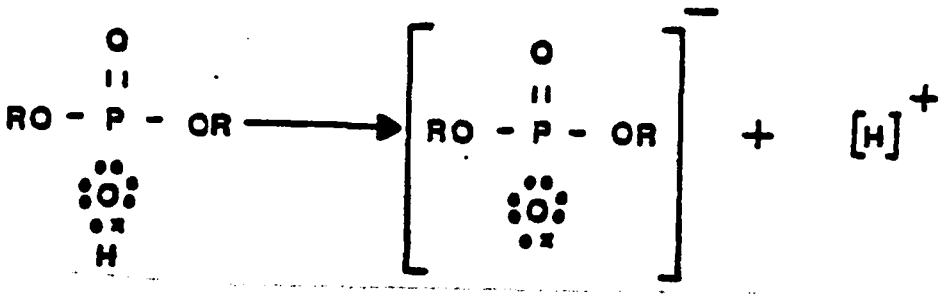

In the above reaction the oxygen atom of the phosphate ester accepts a pair of electrons and thus is a Lewis acid. In terms of Bronsted-Lowry acid-base reactions, the phosphate ester donates a proton and is the acid and the anion is the conjugate base.

Fowkes (18) proposes that interactions between adsorbates and adsorbents can be explained in terms of electron acceptor-donor (acid-base) interactions. Fowkes theory can be readily applied to the barium titanate/phosphate ester system.

The barium titanate and phosphate ester react as follows when in solution with the MEK-ethanol organic solvent

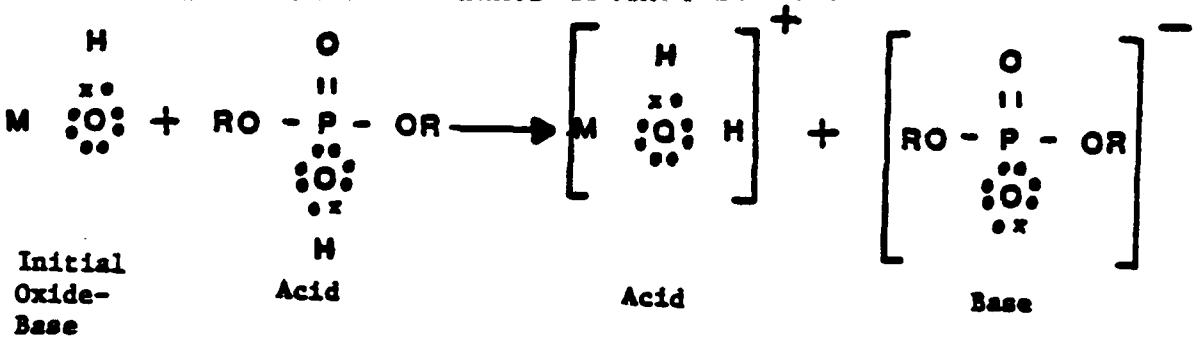

The literature indicates a neutral metal oxide surface is usually represented by a metal-hydroxyl complex (M-OH), thus, the initial barium titanate surface is represented in this fashion.

---

*(x,o) refer to valance electrons as denoted by Lewis formulas

The acidic hydrogen liberated on dissociation of the acidic phosphate ester forms a coordinate bond with the basic metal oxide ($BaTiO^3$) which now becomes the conjugate acid, while the ester becomes a base. The protonated metal oxide and anionic ester can now react. This reaction is explained by a Lewis acid-base reaction.

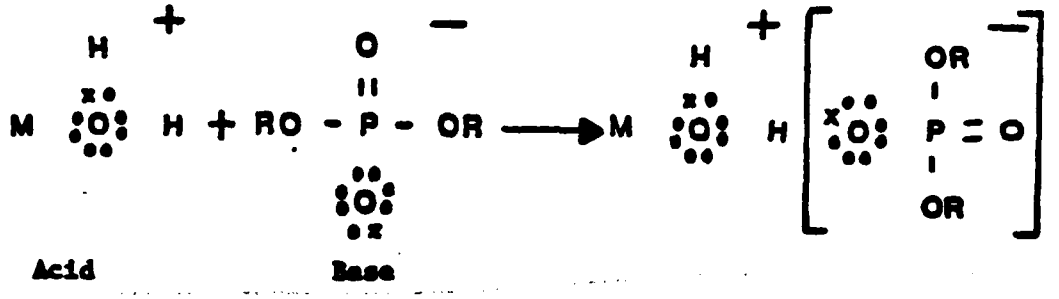

The metal oxide is the electron acceptor, and the anionic ester is the electron donor. The nature of the bond between the anionic ester and the protonated metal oxide complex is probably chemical in nature. The positively charged metal oxide and the anionic phosphate ester attract by electrostatic forces forming an ionic type bond. It should be noted that loosely bound (hydrogen bonded) physically adsorbed molecular water has a definite effect on interactions at the interface as indicated by previously discussed dispersibility measurements.

An electrophoresis test was performed to determine the powder surface charge when added to various liquid systems in order to substantiate the proposed electron acceptor-donor surface adsorption mechanism. The initial charge on the barium titanate surface when added to both aqueous and MEK-ethanol solvent systems was slightly positive as indicated by a slight migration towards the cathode. The surface readily adsorbed positive ions as indicated by a small

increase in pH when added to neutral water. On addition of monovalent acid (HCl) to both the water and the MEK-ethanol systems, a migration towards the cathode occurred indicating adsorption of positive ions, and thus a positively charged surface.

On addition of the HCl to both the aqueous and solvent systems, it was noted that migration of particles towards the cathode was greater in the solvent system than in the aqueous system. Apparently, adsorption of positive ions is greater from the solvent onto the powder surface than from the water onto the powder.

The dispersion of barium titanate-water-phosphate ester showed a strong migration towards the anode indicating a strong negative surface charge. The dispersion of barium titanate-solvent-phosphate ester showed a strong migration towards the cathode indicating a strong positive surface charge. The interesting comparisons between these two systems is that the barium titanate-water-phosphate ester system indicates a negative surface charge, while the barium titanate-solvent-phosphate ester system indicates a positive surface charge.

The following adsorption model is proposed on the basis of lyophobic-lyophilic reactions of polyelectrolytes in an attempt to explain the indicated surface charges on addition of the phosphate ester to the aqueous and non-aqueous systems.

In both the aqueous and non-aqueous systems the phosphate ester dissociates. The liberated proton is attracted to the metal oxide as indicated by acid-base reactions. The anionic portion of the long chain amphipathic polyelectrolyte (phosphate ester), created on dissociation, is attracted by electrostatic forces (coulombic attraction forces) to the positive surface forming an ionic chemical

type bond at the positively charged surface.

In the aqueous system apparently a larger amount of this anionic polyelectrolyte adsorbs on the surface and effectively reverses the charge on the particle. An explanation as to how more than enough electrolyte to neutralize the surface charge adsorbs on the surface is as follows. The nonpolar long chain hydrocarbon tail extends away from the particle surface into the polar aqueous media. The nonpolar hydrocarbon tail is water insoluble (hydrophobic). The hydrophobic tail attracts a hydrophobic tail of another ionized phosphate ester molecule by van der Waals forces as shown in Figure 9. The polar anionic end of the phosphate ester molecule is hydrophilic in the aqueous media and extends into the bulk. In effect, a charge reversal occurs (12). The original positive surface created by adsorption of positively charged protons is reversed by formation of a hemimicelle on adsorption of the amphipathatic phosphate ester. This explains the migration towards the anode on addition of the phosphate ester to the aqueous barium titanate suspension.

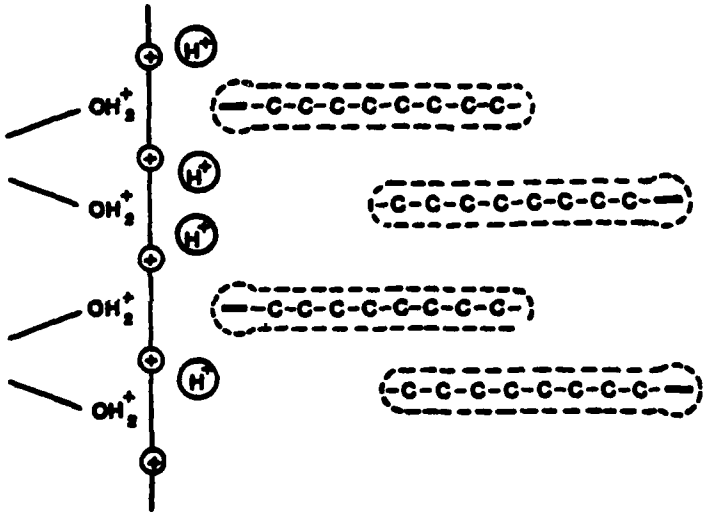

Figure 9. A schematic for the adsorption of the phosphate ester onto the barium titanate surface in an aqueous media showing the formation of a hemimicelle and thus charge reversal.

In the case of the organic system, the anionic end of the phosphate ester is attracted to the positively charged surface by coulombic attraction forces as was the case in the aqueous suspension but only a monolayer of phosphate ester forms on the surface as shown in Figure 10. In the organic media, the hydrocarbon tail is lyophilic and soluble in the relatively nonpolar MEK-ethanol solution, therefore, there is not attraction of additional amphipathatic polyelectrolytes as in the case of the aqueous system.

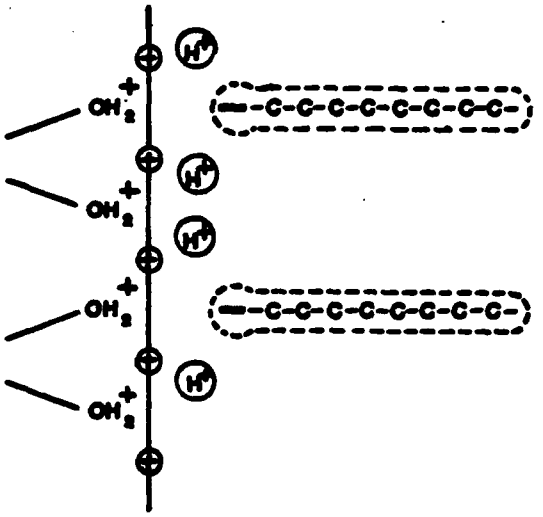

Figure 10. A schematic for the adsorption of the phosphate ester onto barium titanate in the MEK-ethanol azeotrope.

The positive surface charge arose because the negative charge of the anionic end of the phosphate ester is small in comparison to the strong positive surface created by proton adsorption and is not strong enough to offset the positive charge, therefore, the particle migrates toward the cathode.

3.6 Adsorption Isotherms: Phosphate Ester

The isotherm for the adsorption of phosphate ester onto barium titanate was obtained using the powder as received and the MEK-ethanol solvent dried over molecular sieves (absolute ethanol was used for this experiment). It was necessary to remove molecular water which could act as an impurity and in turn affect adsorption. Tormey (4) found water can inhibit solute adsorption while causing a pronounced adsorption maxima in the isotherm. Parfitt (14) notes that impurities at the adsorption interface can cause adsorption maxima, thus making monolayer determination difficult. Also, viscosity curves for the MEK-ethanol-barium titanate system, as discussed previously indicated that the stability of the dispersion increased by using dry components. It becomes apparent from the aforementioned that the presence of water, in most cases, can be detrimental to adsorption observations. It was, therefore, decided to conduct this experiment using dry materials, first.

The as received barium titanate powder contained a relatively a small amount of water (0.123%). Vacuum drying failed to reduce the water content appreciably (0.112%). It is doubtful that surface hydroxyle and strongly bound molecular water could be removed to any great extent by additional drying, therefore, the powder was used as received. Most of the water was contained in the solvents, therefore, these were the components which were further dried.

The adsorbed concentration, Γ , was calculated from the equation

$$\Gamma = \frac{n_o \Delta X_1}{mA}$$

Where n_o is the initial number of moles of solution brought in contact with grams of barium titanate powder of specific surface area A, ΔX, is the change in solution concentration (in mole fraction) of the phosphate ester due to adsorption on the barium titanate

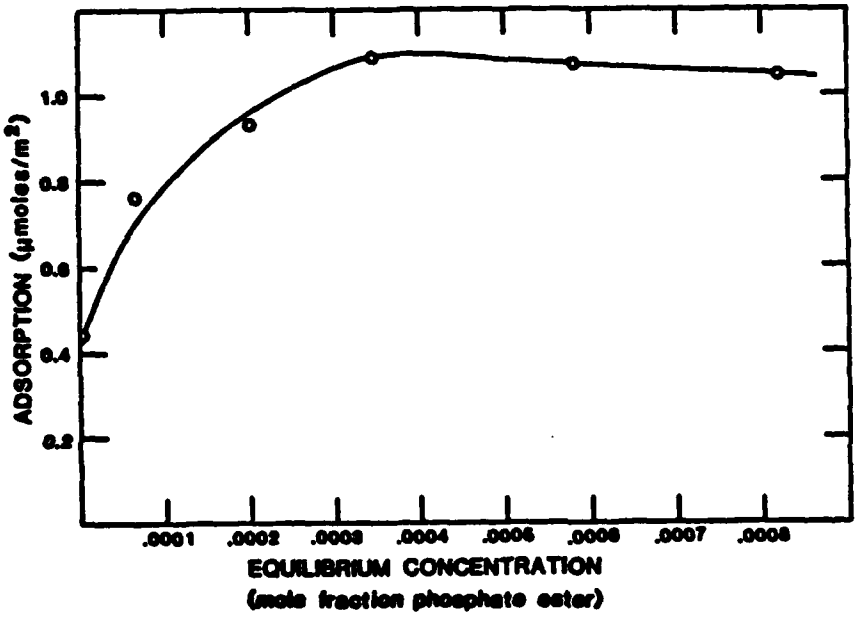

Figure 11. Isotherm for the adsorption of the phosphate ester onto barium titanate powder,

Figure 11 is the adsorption isotherm for the phosphate ester's adsorption onto barium titanate in terms of moles/m^2. The initial slope of the isotherm represents the rate of change of site availability with increasing solute adsorption. As more solute is adsorbed, there is progressively less chance that solute in the adjacent bulk solution will find a suitable site onto which it can be adsorbed. When all of the available surface sites become occupied, saturation of the surface has been reached in the form of

and a lower affinity for the exposed layer of solute molecules already adsorbed and thus does not form a second layer.

Further information can be gathered from the adsorption data by use of the Langmuir equation which can be applied to composite isotherms where the adsorbed layer is confined to a single molecular layer, and the adsorbtion sites are all equivalent. For purposes of plotting the adsorption data, a modified version of the Langmuir equation was used in the linear form (13):

$$\frac{X_1}{\Gamma_1^s} = \frac{1}{\Gamma^s}\left[X_1 + \frac{1}{K-1}\right]$$

The Langmuir plot X_1/Γ_1^s versus X^1 for the adsorption of the phosphate ester onto barium titanate is seen in Figure 12. The slope (s) of the line was used to determine the adsorption at monolayer coverage since $s = 1/\Gamma^s$. The ratio of the slope to the intercept (b) of the line was used to determine the value of K ($s/b = K-1$) from which an estimate of the free energy of adsorption (ΔG^o) was obtained from the following equation:

$$\Delta G^o = -RT\ln K$$

The value of Γ^s calculated from the slope of the line was 1.09 moles/m^2 which corresponds quite well with the plateau level of adsorption seen in figure 11, as it must, due to the form of the equation. The Γ^s value calculated from the slope of the line must be equal to the plateau value when there is a long flat plateau, because when X_1 is large, Γ_1^s approaches Γ^s. Actually, the

Γ^s value calculated from the slope of the line is more useful for determining saturation at a monolayer of coverage for isotherms where a distinct plateau is not seen. The phosphate ester isotherm shows a very long distinct plateau, therefore, Γ^s calculated from the slope of the line has a value almost identical to that of the plateau adsorption level. In our case, the equation is more useful for determining the equilibrium constant K.

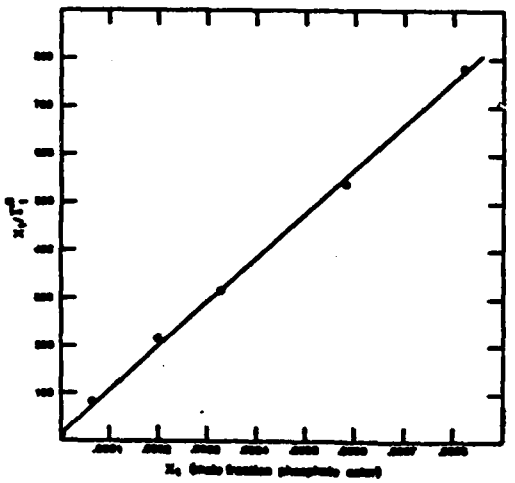

Figure 12. Langmuir plot of X_1/Γ^s versus X_1 for the adsorption of the phosphate ester onto barium titanate

The change in the free energy of adsorption (ΔG^o) calculated from equation 5.9 at 25°C was -6.49 kcal/mole. A negative free energy change indicates spontaneous adsorption and probably can be attributed to the ionic adsorption of the negatively charged phosphate ester ($P-O^-$) onto the protonated barium titanate surface to form a $BaTiO^+H^{-2}OP$ linkage. The free energy values obtained here are similar to those reported by Tormey (4) for the adsorption of glycerol trioleate from toluene onto alumina, which ranged from -6.4 to -6.8 kcal/mole, and seem acceptable when considering the fatty acids are adsorbed by a combination of hydrogen bonding and ionic mechanisms.

a monolayer, and no further adsorption can take place unless new surface sites are made available. Additional approaching solute molecules are subsequently repelled from the surface. Monolayer coverage is indicated by a long, flat plateau on the adsorption isotherm. The plateau is seen to initially occur in Figure 11 for the barium titanate phosphate ester system at an equilibrium concentration of 0.00035 mole fractions and an adsorption surface excess of 1.09 moles/m^2 of phosphate ester. The adsorption plateau in Figure 11 indicates there is no further adsorption of the phosphate ester beyond a monolayer of coverage.

For the adsorption of phosphate ester onto the barium titanate, it can speculated that the positively charged adsorbent, is partially neutralized by the adsorption of the oppositely charged phosphate ester molecule converting the surface from one of high energy to one of lower energy, thereby reducing the driving force for further adsorption beyond a monolayer of coverage. The anionic ends of the phosphate ester are held by ion-ion attraction to the positively charged barium titanate surface, and this, when monolayer coverage is complete, presents to the adjacent bulk solution a new surface of lyophilic hydrocarbon segments which are less attractive to the approaching phosphate ester anions than the original surface. Thus adsorption of additional layers is inhibited.

Another possible explanation for the existence of a long plateau is that a high energy barrier must be overcome once monolayer coverage is complete before additional adsorption can occur on new sites. Furthermore, at a monolayer of coverage, where no additional adsorption occurs, the solute has a higher affinity for the solvent or for other solute molecules in the bulk solution

A comparison of Tormey's (4) adsorption isotherm for the glycerol trioleate to the isotherm for the phosphate ester shows in general that the initial monolayer covered for the glycerol trioleate occurred at approximately 0.4 to 0.6 mg/m^2 at an equilibrium concentration of approximately 0.4 wt % (Tormey measured the adsorption of the fatty acid on various types of alumina), while a monolayer coverage for the phosphate ester occurred at 0.8 mg/m^2 (1.07 $moles/m^2$) at an equilibrium concentration of 0.4 wt%. These results appear to be similar. Tormey also measured the adsorption of Menhaden fish oil on various aluminas and reported monolayer coverages of approximately 1.5 mg/m^2 at an equilibrium concentration of approximately 0.8 wt %. These figures indicate adsorption was three to four times greater forthe fish oil than for the phosphate ester or the glycerol trioleate.

Tormey (4) suggested that the glycerol trioleate adsorbed with a horizontal surface orientation while the fish oil adsorbed with a vertical orientation. (The fish oil may adsorb beyond a monolayer.) The vertically oriented molecules had a lower surface area coverage per molecule than the horizontally oriented molecules. It can be suggested from these results that vertical orientation allows for more molecules to be adsorbed per unit area of surface than horizontal orientation, thus allowing more fish oil to be absorbed than glycerol trioleate.

From monolayer adsorption values for the phosphate ester, it was determined the phosphate ester occupied 152 $Å^2$ per molecule. The phosphate ester used in this study contained equal amounts of both the mono- and dialkylated phosphate esters in a tetrahedral configuration. From molecular models, it can be estimated that if

the monoalkylated phosphate ester adopts a horizontal orientation where the phosphoryl group as well as the hydrocarbon chain are in contact with the oxide surface, the area occupied would be approximately 140 $\AA^2$ per molecule. Vertically oriented molecules, where just the phosphoryl group is in contact with the oxide surface and the hydrocarbon chain extends perpendicular from the surface into the bulk solution, occupy an area of only approximately 12 $\AA^2$ per molecule. For dialkylated phosphate esters, where both hydrocarbon chains lie horizontally on the surface, the model predicts an area of approximately 280 $\AA^2$ per molecule. The molecular area determined from adsorption values at monolayer coverage (152 $\AA^2$ /molecule) suggests that at least one hydrocarbon chain must be oriented horizontal to the oxide surface. For dialkylated molecules this suggests that one hydrocarbon chain is at least partially horizontal to the surface due to tetrahedral bond angles, while the other chain extends vertically into the bulk, or both chains may be oriented partially vertical to the surface. Possible configuration are loops, coming out and returning to the surface or tails extending into the solvent or some combination of loops, tails and horizontal adsorption.

The 152 $\AA^2$ per molecule calculated from adsorption values is somewhat greater than areas predicted from molecular models. It is doubtful the phosphate ester molecules would adsorb in a close packed arrangement due to possible coiling of the vertically oriented hydrocarbon chains that would inhibit additional approaching molecules from attaching onto available surface sites. Also the shape of the adsorption isotherm suggests the possibility of co-adsorption of solvent or impurities along with the solute

which would prevent close packing. The isotherm shows a slight decrease in the plateau level as concentration increases beyond the initial monolayer adsorption value. A maxima in the plateau level followed by a slight decrease in adsorption is often attributed to solvent co-adsorption (14) and/or impurity adsorption (4). In our case, impurity adsorption would most likely be in the form of molecular water. The adsorbed surface water can inhibit solute adsorption by blocking availably surface sites and thus prevent close packing.

3.7 Dispersion Stability

An interesting correlation can be drawn between the concentrations of phosphate ester at which monolayer coverage and minimum viscosity occurred. Monolayer coverage and minimum viscosity both occurred at a similar concentration of phosphate ester. It should be noted that the aforementioned tests were conducted at different solids, fractions, nevertheless, it was found that the apparent minimum viscosity at various concentrations of solids occurred at almost identical proportions of phosphate ester, the apparent minimum viscosity occuring at approximately 0.8 vol % phosphate ester corresponds to the equilibrium concentration of approximately 0.0006 mole fractions. Figure 13 indicates that this corresponds to the equilibrium concentration where monolayer coverage was initially established. It can be concluded for the phosphate ester barium titanate system that a monolayer of coverge corresponds very well with maximum dispersion stability and minimum agglomeration. Before the onset of a monolayer of coverage and minimum viscosity, there are not enough solute molecules adsorbed onto the surface to provide a repulsive force necessary to prohibit particle-particle contact. It can be proposed that beyond the concentration of solute at which monolayer coverage occurs co-adsorption of solute (14), reorientatin of adsorbed material (13), or the collapse of the possible electrical double layer may account for the increase in viscosity and agglomeration of particles.

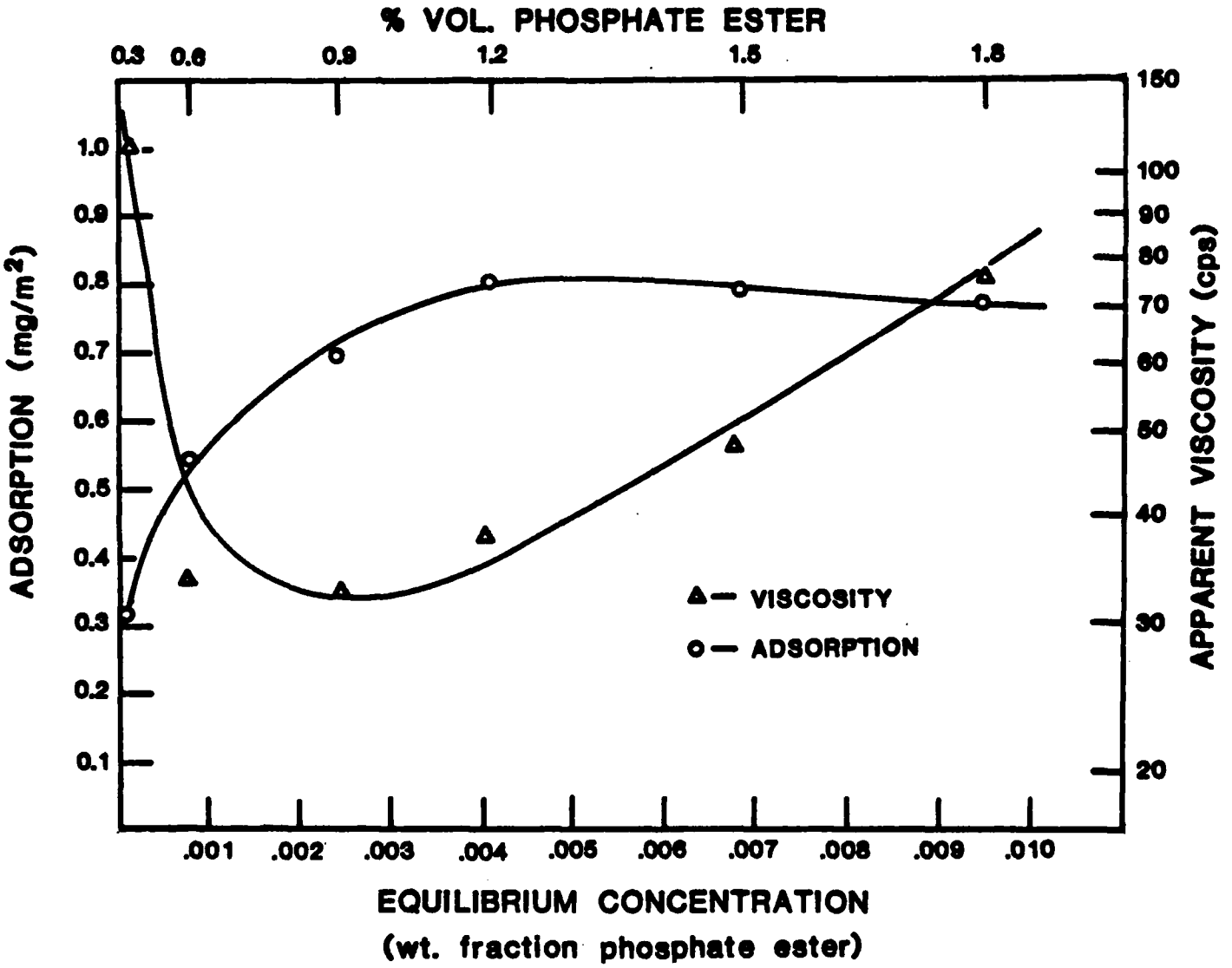

Figure 13. Viscosity curve (Figure 1) overlayed on the adsorption isotherm such that the concentrations of phosphate ester prior to adsorption match.

The primary stabilizing mechanism, whether electrostatic or steric, cannot be determined from experimental evidence gathered to date. In favor of the electrostatic mechanism is the strong charge which is imparted to the particles upon addition of the phosphate ester. On the side of steric hindrance is that the phosphate ester forms a long chain which probably takes on, at least a particl verticle orientation and the steric mechanism supplies the repulsive force. Although a decade ago most investigators believed that because of the low dielectric constants of organic solvents and low electrolyte concentration, the double layer width was very large and offered little repulsive barrier, however, increasing evidence suggests electrostatic repulsion as being important in non-aqueous solvent systems. Fowkes (15) has further suggested the optimum stabilization occurs by a combination of steric stabilization for short range repulsion and electrostatic for slightly longer range repulsion.

During the coming year, additional experiments will be performed to determine the nature of the important stabilization mechanisms. Electrophoritic measurements will be made as a function of electrolyte concentration and an effort will be made to determine the thickness of the coverage of the polyelectrolyte to obtain a quantitative estimate of the steric stabilization contribution.

3.8 Green Tape Density

Finally, the phosphate ester, was used in an effort to maximize the particle packing of the cast tape. It is well known that the sinterability of a powder compact is dependent upon the degree to which the powder particles are packed together. The degree of

particle packing in the barium titanate tapes can be indirectly measured by determining the bulk density of the cast green tapes (16).

In order to cast high density tapes, it is first necessary to maximize solids loading in the casting slip. The highest loading can be achieved at the point of maximum dispersion. Therefore, a concentration of phosphate ester versus viscosity curve was generated for the casting system as seen in Figure 14.

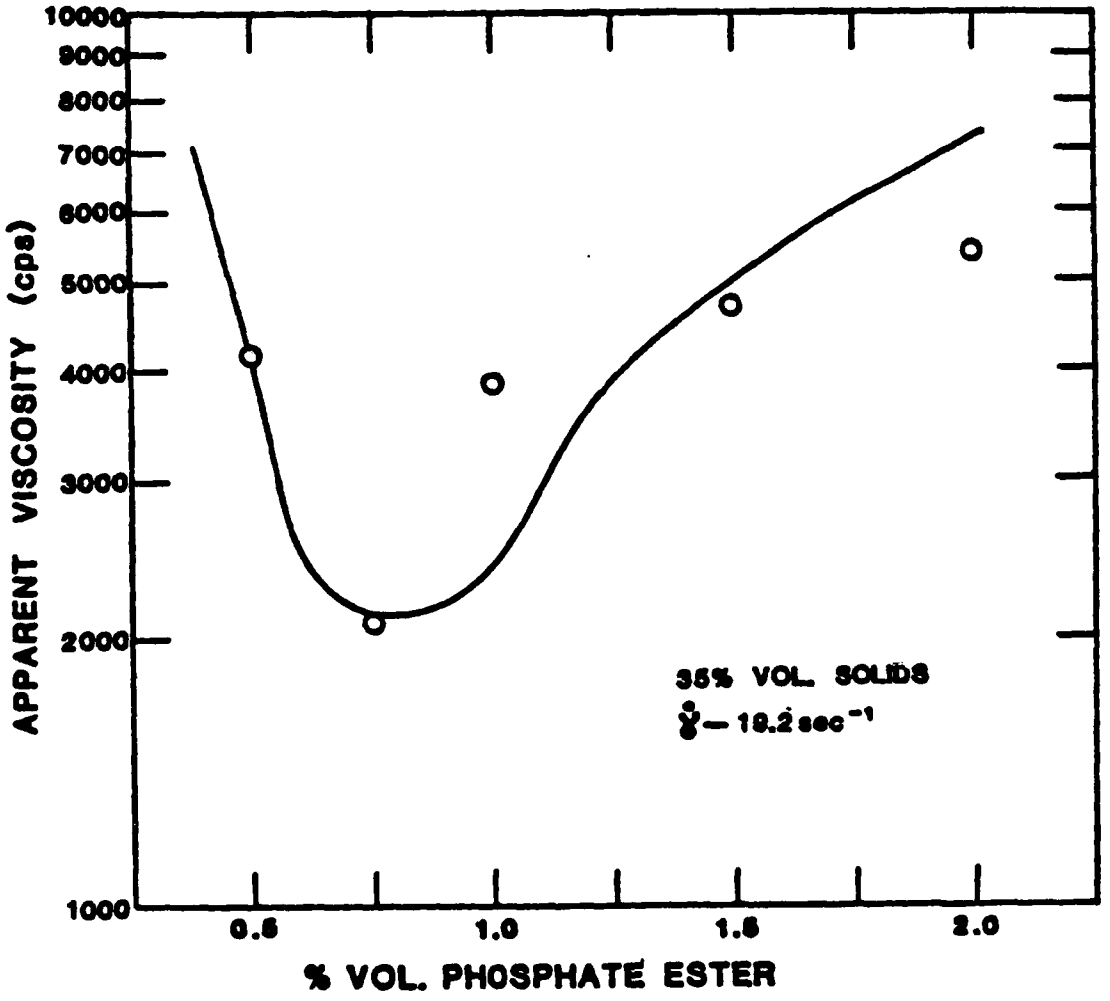

Figure 14. Apparent viscosity as a function of phosphate ester concentration for the tape casting slip.

The point of maximum dispersion for the casting system (including binders, plasticizers, etc.) occurred at a concentration of approximately 0.7 vol % for a 35 vol % solids dispersion. 0.7 vol % of phosphate ester was subsequently used as the concentration required to produce maximum dispersion in the casting system. At this concentration, the phosphate ester allowed for the casting of slips as high as 45 vol % solids. This ability to cast at high solids fractions was subsequently responsible for high bulk densities achieved in the cast tapes compacts.

Green tapes dispersed by the phosphate ester had an average bulk density of 3.52 g/cm^3. Weight loss after firing indicated that 7.87% of the total weight can be attributed to organic materials, therefore, 92.13% of the 3.52 g is the barium titanate. The bulk density of the barium titanate itself is then 3.24 g/cm^3. This is 55% of the theoretical density (5.90 g/cm^3 as indicated by helium pycnometry).

Tolino (17) made tapes using a composition and processing method identical to the one used in this study, except fish oil was used as a dispersant. His study allowed us to compare the bulk densities obtained when using the phosphate ester as a dispersant to those obtained when using the fish oil as a dispersant. Tolino was only able to cast tapes from slips at 30 vol % solids when using the fish oil as a dispersant which was evidentally responsible for lower bulk densities in the cast tapes. Tapes dispersed by the fish oil had a bulk density of only 2.97 g/cm^3. After binder burn out, the bulk density of just the barium titanate is 2.63 g/cm^3 which is 44.67% of theoretical density. This density is quite a bit lower than the densities achieved when using the phosphate ester.

Tapes dispersed by the phosphate ester were subsequently sintered at 1400°C. Figure 15 shows the surface of the fired tape. Grain growth is uniform and porosity appears to be minimal.

Viscosity measurements using fish oil as a dispersant are compared with those for the phosphate ester in Figure 16. The minimum viscosity using the fish oil is a factor of approximately 20 times higher than that for the phosphate ester which accounts for the inability to disperse a higher loading of powder into the solvent. More recent measurements which will be published in a future report indicate that the fish oil is not very soluble in ethanol and it is the presence of the ethanol which reduces the effectiveness of the fish oil. The fish oil appears to be a slightly more effective dispersant in MEK alone than is the phosphate ester.

Figure 15. SEM micrographs of sintered tape surfaces for tapes fired using the phosphate ester as a dispersant.

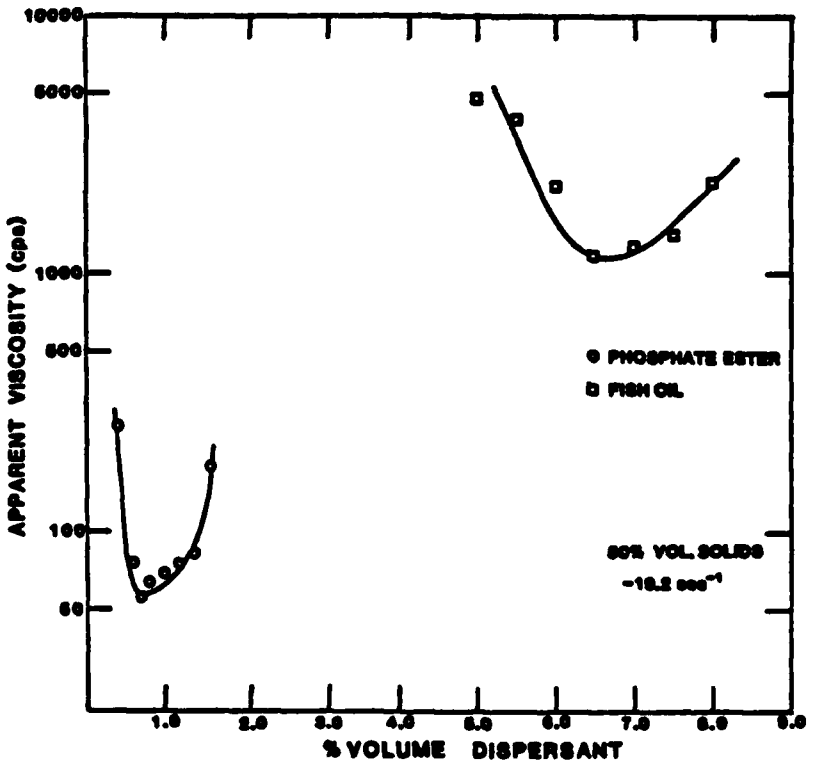

Figure 16. Apparent viscosity as a function of phosphate ester and fish oil concentrations.

3.9 Green Tape Strength

The ultimate tensile strength of green tapes was measured as a function of method of drying, type of dispersant and sequence of dispersant addition.

The tensile strength was determined using a Universal testing machine with 25 psi pressure grips. These grips were found to cause less sample tearing than mechanical grips. The dog-bone sample shape shown in Figure 16 was adoped avoid failure at the grips. Initially, the effect of loading rate was determined for samples consisting of (by volume) 35% $BaTiO_3$, 33.25% MEK-Ethanol azeotrope, 20% Acryloid B-7, 5% Carbowax 100, 5% Santicizer 160, 1% cyclohexanol and 0.75% Emphos PS-21A. Measurements were made at 6 different cross heat speeds.

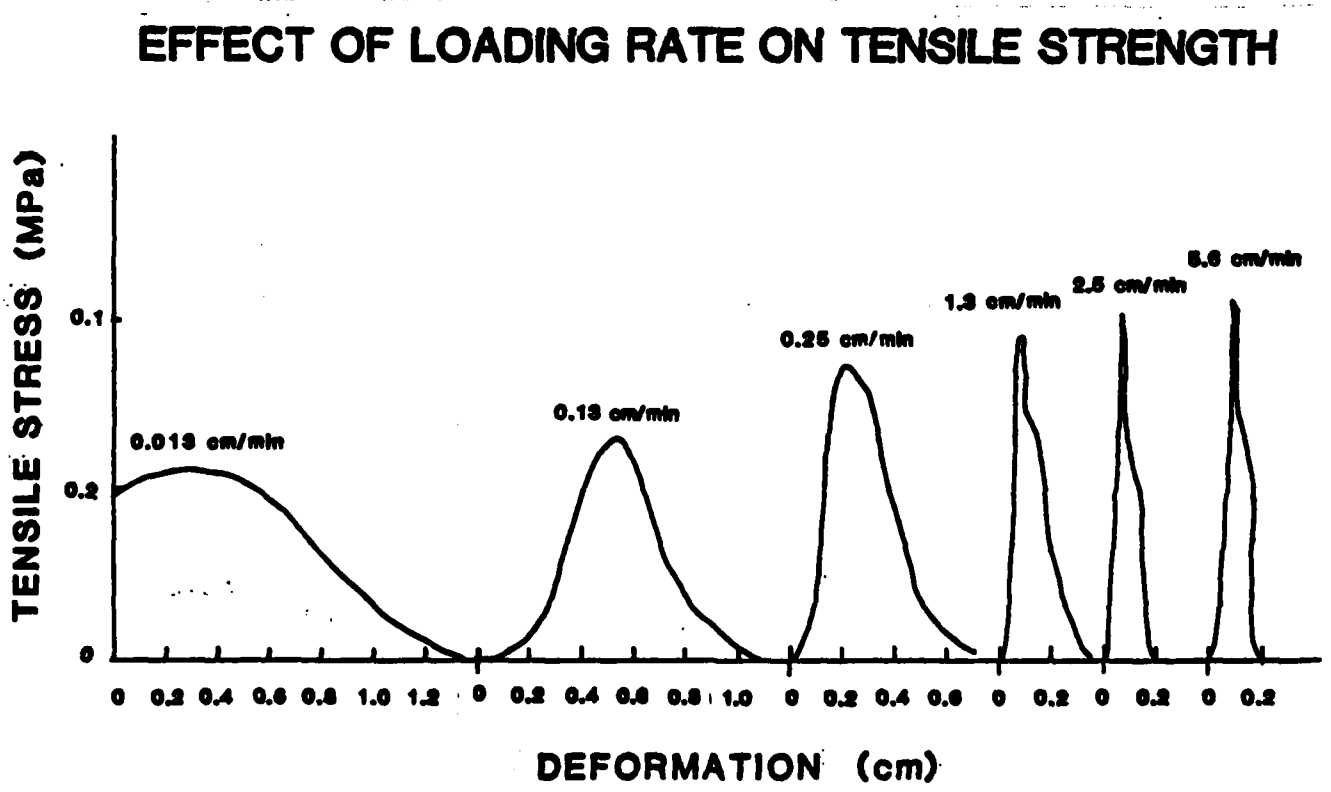

Figure 17. Tensile load vs deformation curves for several different loading rates.

Figure 17 shows tensile strength vs. deformation curves for loading rates of 0.013, 0.13, 0.25, 1.3, 2.5, and 5.6 cm/min. As expected slow cross head speeds yielded lowering ultimate tensile strengths with greater overall deformation. Conversally faster loading rates yielded higher tensile strengths with less total deformations. The green tapes can be considered a ceramic-polymer composite consisting of ceramic particles in a continuous polymeric matrix. Hence the properties of the polymer matrix dominate the mechanical properties of the composite. Increasing loading rate is analogous to decreasing the temperature of the test. When the temperature is high, i.e. above the glass trnasition temperature, the polymer behaves as a viscous liquid and deformation is large. This corresponds to a slow loading rate. On the other hand, if the temperature is below the glass transition temperature, the polymer behaves as a brittle material and overall deformation is small, corresponding to a fast loading rate.

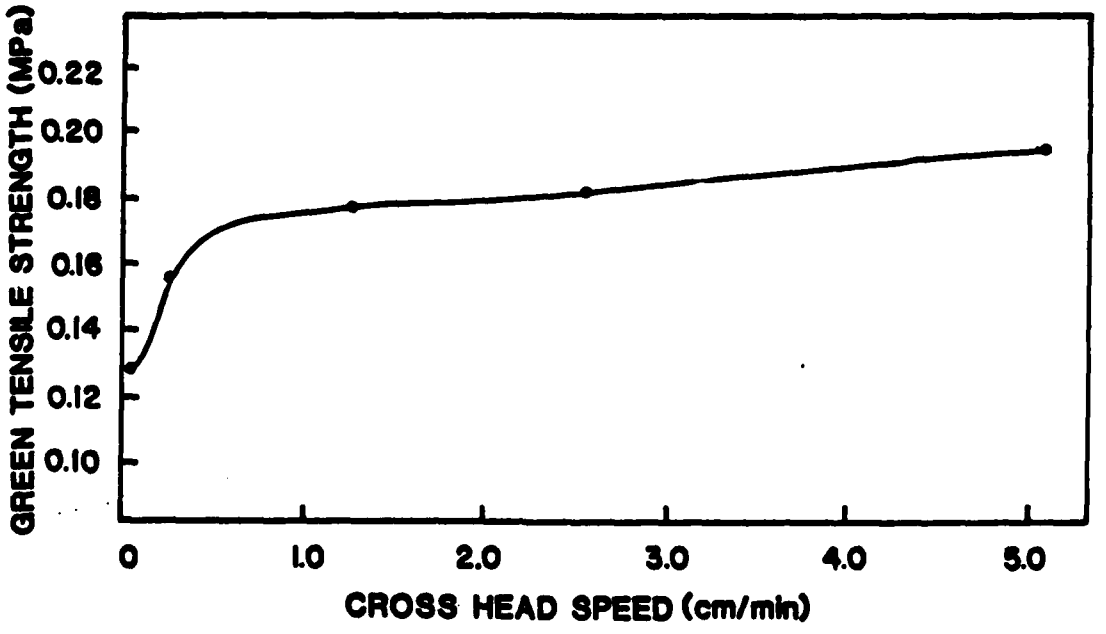

Figure 18. Ultimate tensile strength of green tapes vs cross head speed.

In Figure 18, the ultimate green tensile strength vs. loading rate is plotted. All subsequent strength data is reported at 2.5 cm/min. which lies in the linear portion of this graph.

Many forming methods such as pressing of extrusion create laminations and residual stresses which tend to weaken the material in one particular direction strength. Uniformity of our tapes were tested, with respect to direction and locations. Samples were cut both perpendicular and parallel to the casting direction, as shown in Figure 19. Strengths were found to be 0.155 and 0.156 MPa respectively. Samples were also cut in various regions of the tape and uniformity was found throughout.

The effect of aging on green tensile strength of cast types was studied. Some samples were aged in contact with the casting glass and others were removed often with a minimum drying time of one hour. Green tensile strength vs. aging time for samples which were not removed from the casting surface until immediately prior to testing is shown in Figure 20. Tensile strength decreases with aging time and there is a large amount of scatter in the data, as evidenced by the large error bars. We postulate that the bottom surface of the tape adhere to the glass casting surface and dries at a slower rate than the exposed upper surface. This places the top surface in a state of tension which produces fatigue cracks, lowering strength. Since these flaws would generally not be of uniform size they would also account for the spread in the data.

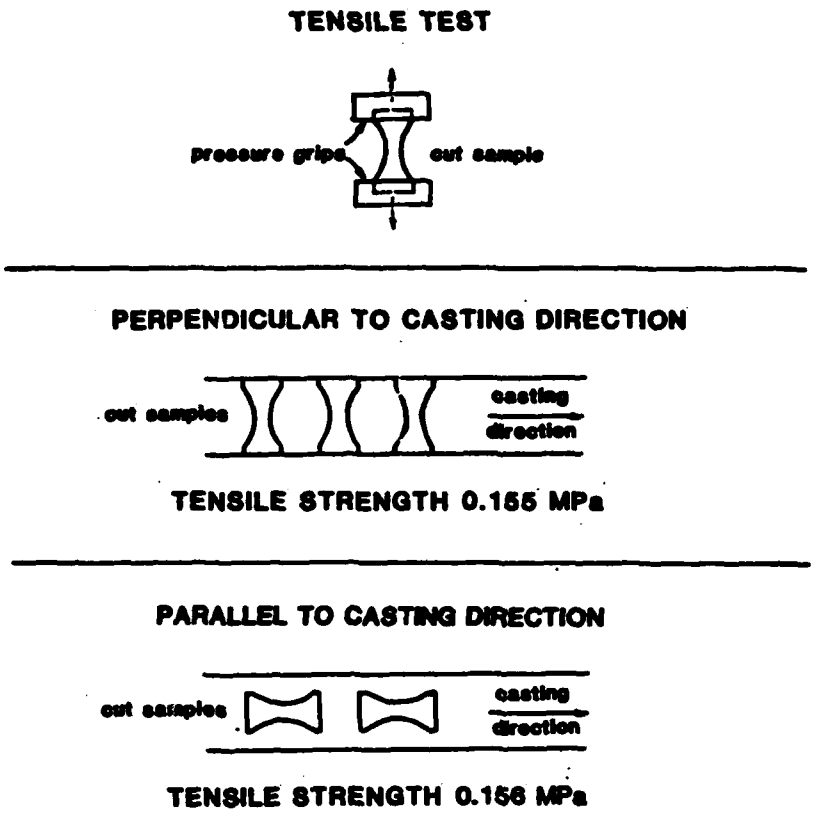

Figure 19. Ultimate strength versus casting direction.

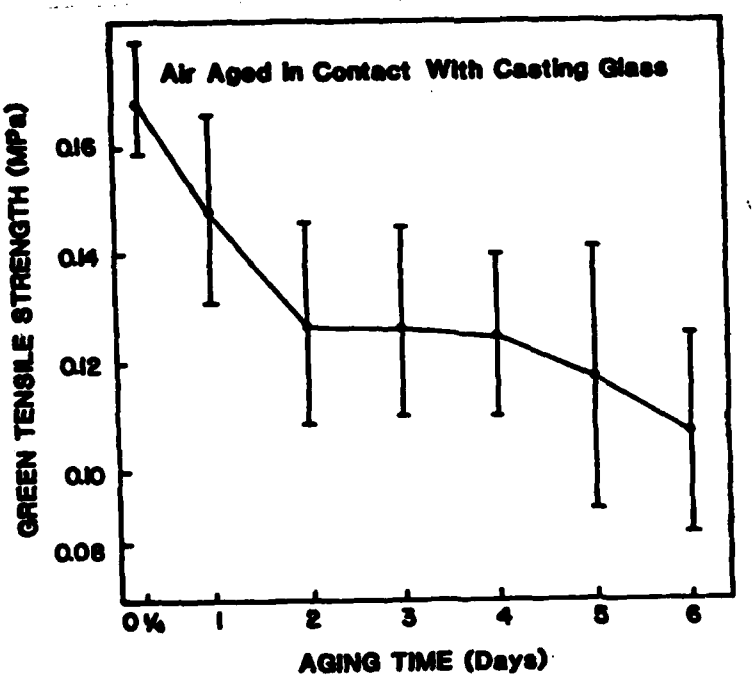

Figure 20. Ultimate strength vs aging time on the glass plate use casting.

To minimize this effect samples were removed from the casting glass after one hour of drying. One hour was the minimum drying time for safe handling of the tape. Tensile strengths were measured for times up to 12 days and were found to increase with an increase in aging time, as shown in Figure 21. Initially, the green tapes have low tensile strengths due to residual unevaporated solvent. As the tapes age, the solvent evaporates causing the particles to approach one another increasing strength. A much smaller deviation, as indicated by the error bars, was observed. This indicates a more uniform flaw size distribution.

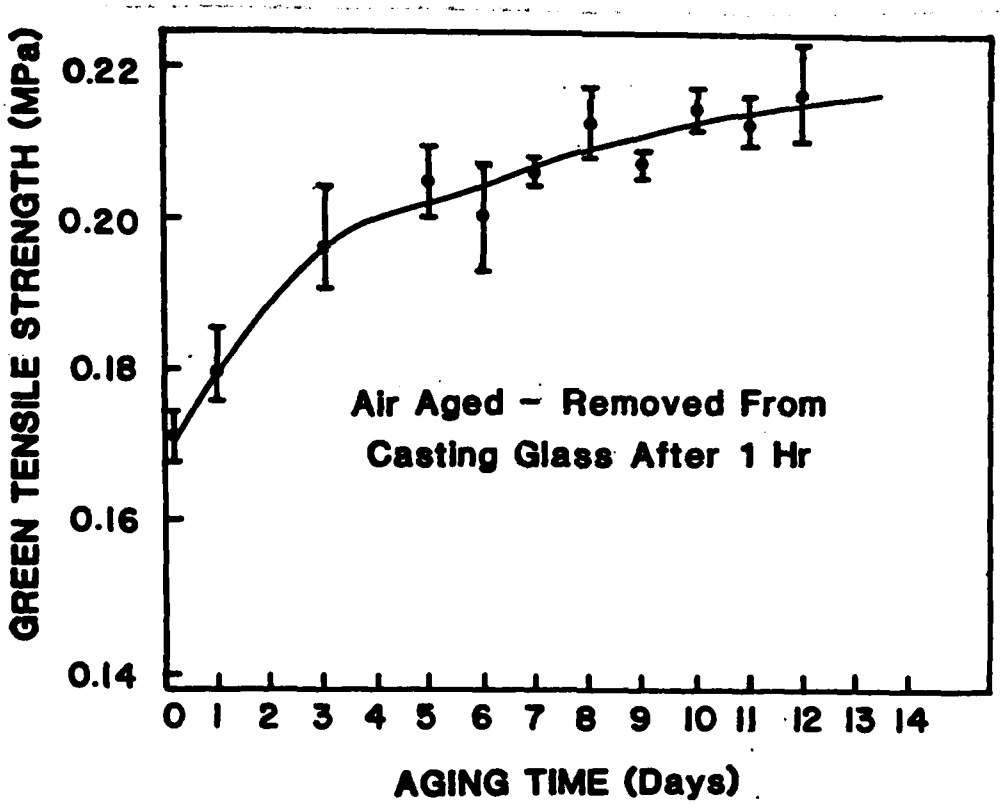

Figure 21. Ultimate strength of tapes removed from the glass plate after one hour and allowed to dry in open air.

The effect of storage method on green tensile strength is shown in Figure 22. Samples were removed from the casting glass after one hour and subsequently stored for up to 13 days open to the air, in a closed container, and in a desiccator. The tapes stored in the desicator had lower tensile strengths than those stored open to air or in a closed container. We postulate that this is due to the desiccant removing water vapors from the tapes. It is believed that water vapor acts as a plasticizer in keeping the tapes flexible and strong. Tensile strengths were slightly lower in the closed container samples than those stored in open air. We attribute this difference to slower drying rate, and possibly water pickup from the air.

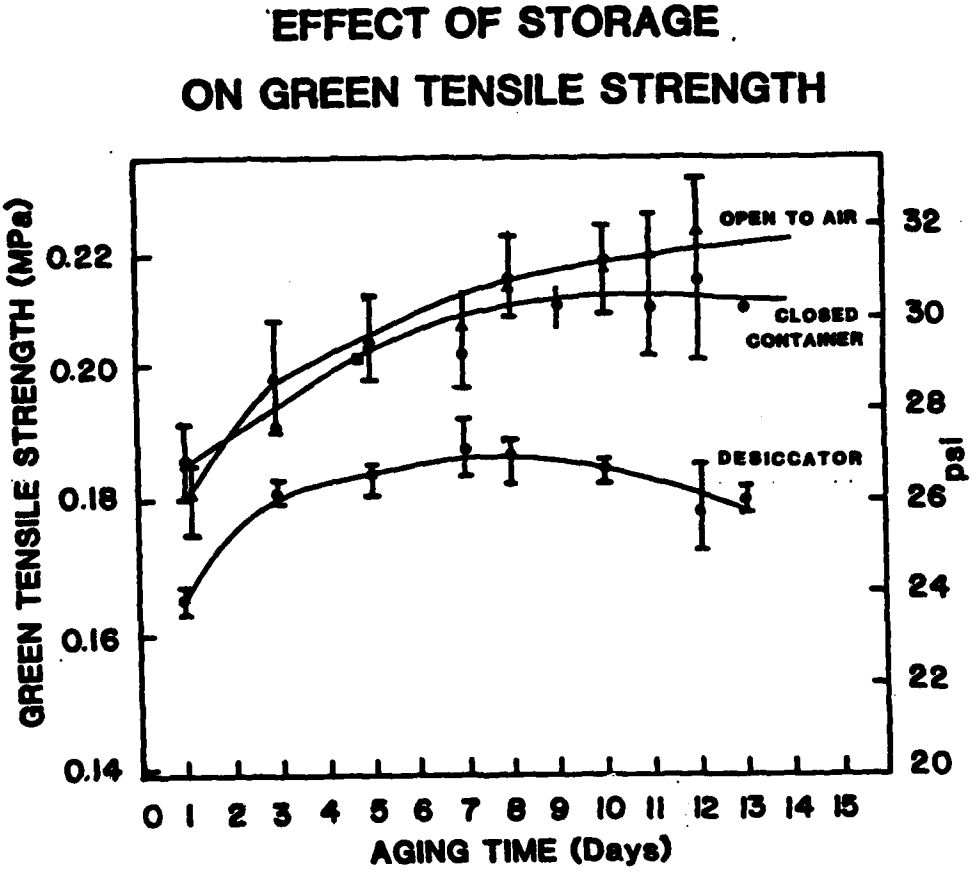

Figure 22. Ultimate tensile strength of tapes removed from the glass plate after one hour and allowed to dry under various conditions.

Table IV shows tape thickness, green density and strength for tape prepared with the three most effective dispersants. Emphos PS-21A Zonyl A**, and Menhaden Fish Oil 2-3. Thickness and tensile strength do not appear to vary significantly. Density was found to be greatest for tapes made with Emphos PS-21A and least for those with Zonyl A. The green densities are lower than reported in the previous section, possibly because a lower solids loading was used here but also possibly because green densities are difficult to measure on such thin green tapes. Slight differences in pressure applied to the micrometer may easily affect the value by as much as 10%. Values listed in Table IV were made by a single experimenter who was different from the experimenter of the previous section which may account for the differences.

Table IV. A comparison of properties of cast tapes using various dispersants.

	Thickness	Density	Tensile Strength
EMPHOS PS-21A	0.017 cm	2.88 g/cc	0.188 MPa
FISH OIL Z-3	0.018 cm	2.77 g/cc	0.183 MPa
ZONYL A	0.017 cm	2.67 g/cc	0.189 MPa

3.10 Order of Addition of Dispersants

Two different orders of addition of components were used: 1) Solvent-binder-powder-homogenizer-plasticizer-dispersant and 2) Solvent-dispersant-powder-binder-plasticizer-homogenizer. The former was always used in the previous section, Section 3.9. The order of addition should particularly effect viscosity since if the binder is added first, it must desorb before the dispersant can adsorb onto the surface. Desorption is often difficult.

Initially, samples were prepared containing 35 volume percent $BaTiO_3$ in the MEK-Ethanol azeotrope varying amounts of dispersant in order to determine the amount of dispersant corresponding to the minimum viscosity. Log viscosity versus volume percent of emphos PS-21A for the powder-solvent dispersant system is shown in Figure 23.

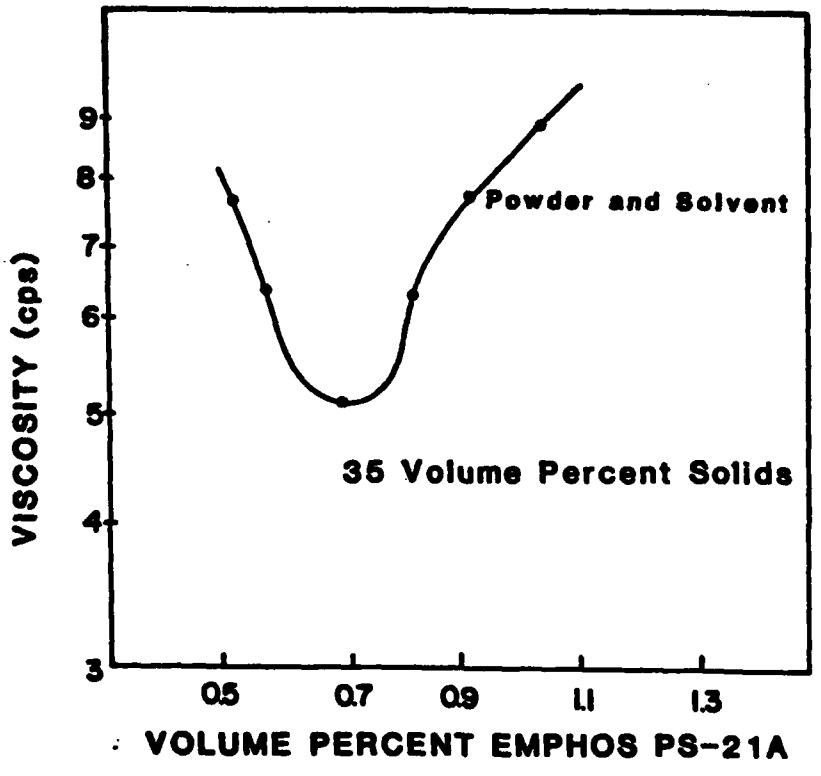

Figure 23. Viscosity versus concentration of the phosphate ester for a powder-solvent suspension containing 35 vol. % solids.

The minimum viscosity occurred at 0.70 volume percent emphos PS-21A. For the system containing powder, solvent, binders, plasticizers, homogenizers, and dispersant, (PSBPH), the viscosities were too high to be measured at the same stress rate (384 sec^{-1}) as the previous samples. In order to compare results at this shear rate it was necessary to extrapolate using a log shear rate vs. log shear stress plot, as shown in Figure 24.

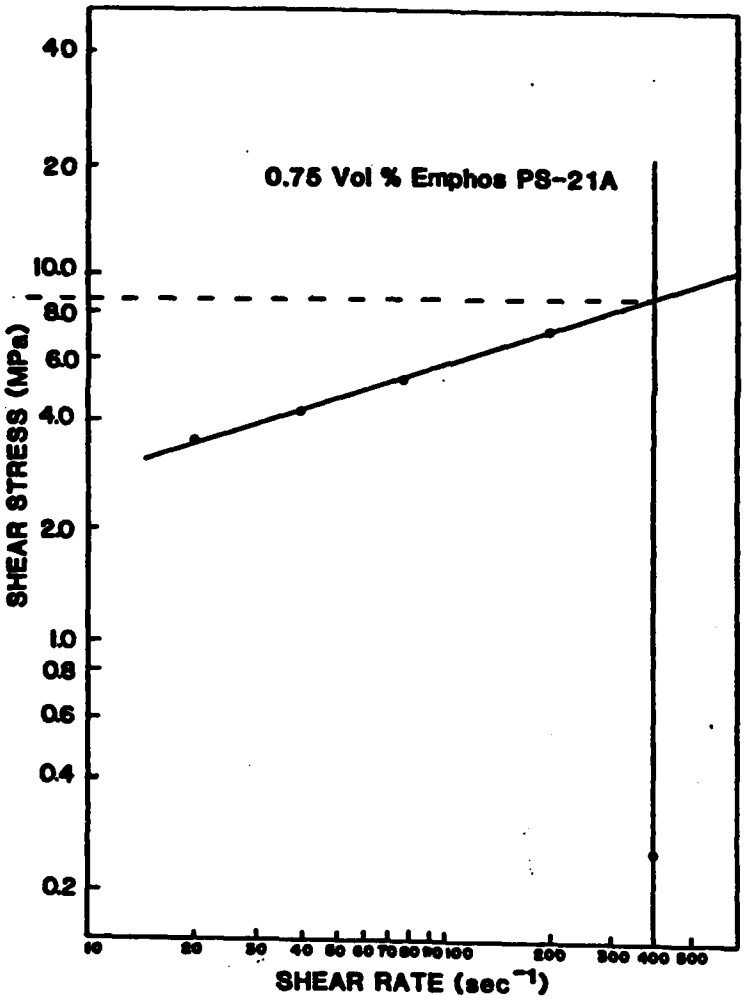

Figure 24. An example of the log shear stress versus log shear rate plots necessary to determine the viscosity at 400 sec-1.

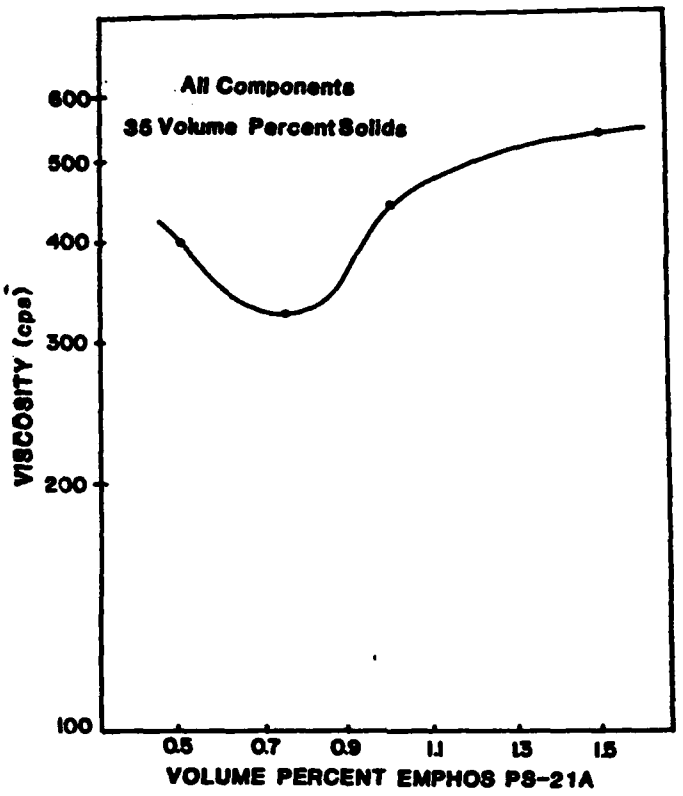

Figure 25. Viscosity vs. concentration of the phosphate ester of suspensions containing solvent, binder, powder homoganizer and plasticizer. Dispersant was added last.

The linearity of the plot allowed this extrapolation, and extrapolated values were used in all subsequent calculations. Figure 13 shows viscosity vs. value percent emphos PS-21A for the solvent-binder-powder-homogenizer-plasticizer-dispersant system. The minimum viscosity of 320.3 centipoise occurred at 0.75 volume percent emphos PS-21A. In order to determine what interference other organics had upon the effectiveness of the dispersant and in order to test the effect of order of addition a relative viscosity was determined. Relative viscosity is a

$$_{rel} = \text{suspension/ fluid components.}$$

A value of 0.814 cps was used for the azetrope (measured with a capilary viscometer) and 32 cps for the solvent-binder-plasticizer-homogenizer system. If relative viscosity of the powder solvent

binder (PSB) and powder-solvent-binder-plasticizer homogenizer (PSBPH) systems are plotted in this way and there is no competition for adsorption sites the relative viscosities should be approximately equal. As shown in Figure 25 this is not quite the case. For the solvent-binder-powder-homogenizer-plasticizer-dispersant system the relative viscosity is greater when the dispersant is added last because the binder has taken up some of the adsorption sites on the powder surface. For the powder-solvent-binder system, component additions order makes little or no difference in terms of relative viscosity since no binder is present to compete with the dispersant for adsorption sites.

Tensile strength measurements were performed on two sets of green tapes: (1) solvent-binder-powder-homogenizer-plasticizer-dispersant and (2) solvent-dispersant-powder-binder-plasticizer-homogenizer. The average strength of (1) was 0.197 MPa and (2) was 0.188 MPa indicating a slightly improved strength when the dispersant was added last. Since the standard deviation was approximately 0.01 MPa the result is apparently significant.

An explanation for this behavior is that when the binder was added first, it had the opportunity of adsorbing onto the surface before the dispersant was added. If the dispersant was added, last the binder could not easily displace the dispersant. The lack of direct attachment of the binder to the particles decreases strength.

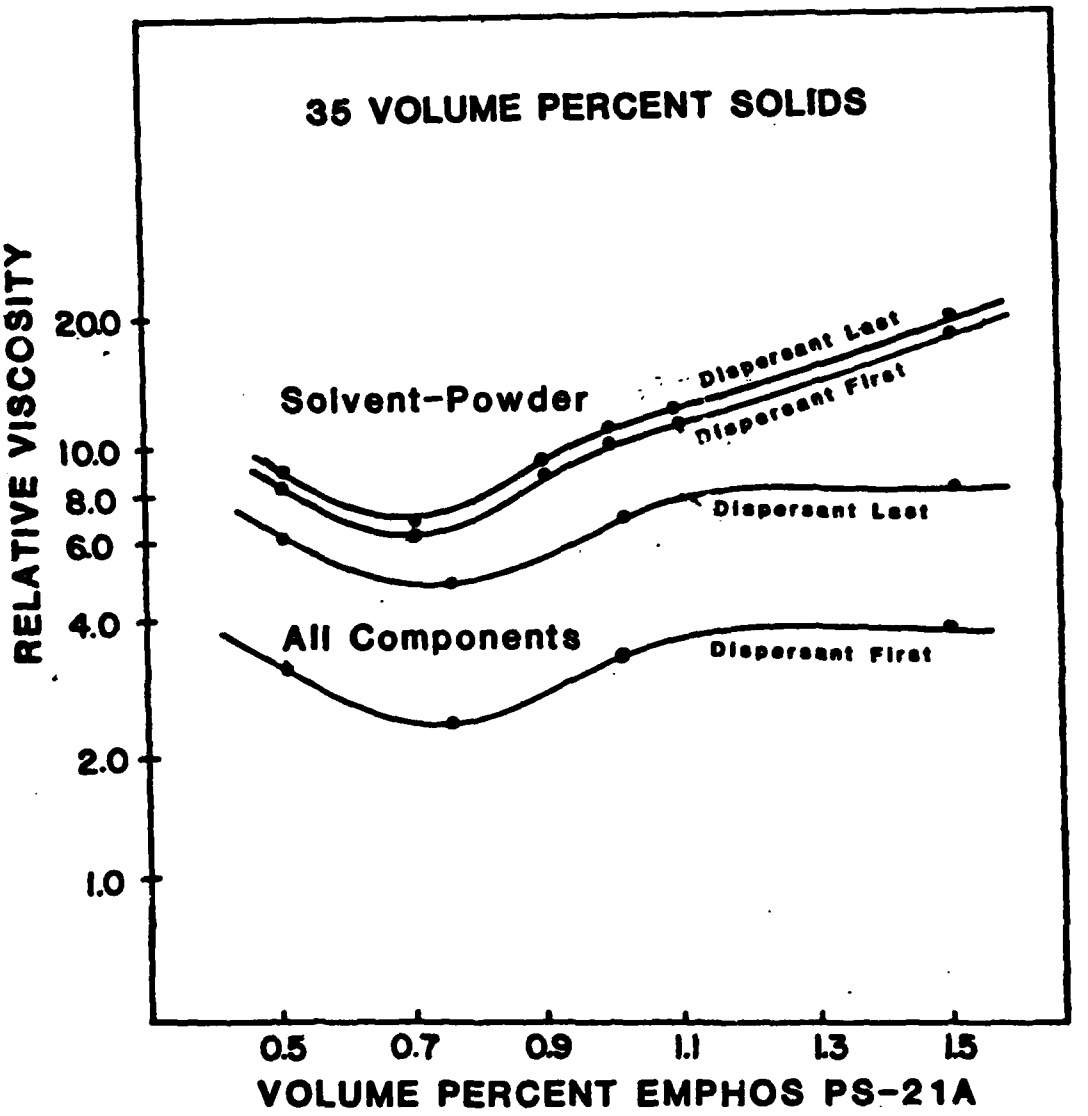

Figure 26. Relative viscosity as defined in text vs. phosphate ester concentration for solvent powder suspensions and solvent, binder, powder, homoganizer, plasticizer and dispersant suspensions.

IV. CONCLUSIONS

The conclusions which can be drawn from this study are as follows:

1. Of the commercial dispersants tested in this study, a phosphate ester is the most effective dispersant for dispersing barium in an azeotrope of methyl ethyl ketone and ethanol followed by Menhaden fish oil. The ethoxylate was effective but has not been thoroughly studied yet.

2. Suspensions dispersed with the phosphate ester at 50 vol % barium titanate had a maximum degree of dispersion at a dispersant concentration of approximately 0.7 vol %. Water was found to have a detrimental affect on the degree of dispersion. Water adsorbed onto the particle surface may block active surface sites and inhibit dispersant adsorption. Co-adsorption of water along with the dispersant may also decrease stability. The use of dry materials along with an aging of the dispersion were found to increase the degree of dispersion of the suspension.

3. Minimum viscosity and maximum packing fraction as a function of phosphate ester concentration both occurred at approximately 0.7 vol % of phosphate ester. Packing fractions of 0.63 were obtained on casting suspensions using the phosphate ester as a dispersant at the same concentration.

4. All suspensions dispersed with the phosphate acted as shear thinning-thixotropic bodies. Degrees of shear thinning and thixotropy were dependent on the degree to which the suspension was dispersed. Fully dispersed systems showed the least amount of shear thinning and thixotropic behavior.

5. An adsorption model for the phosphate ester-barium titanate system was proposed on the basis of acid-base reactions. Adsorption at the solid/liquid interface occurs by means of an ionic adsorption mechanism where the positive particle surface ($M-OH^{+}_{2}$) reacts with the anionic portion of the phosphate ester ($P-O^{-}$) molecule forming a strong ionic type bond. The lyophilic hydrocarbons portion of the molecule subsequently extends into the bulk imparting a steric barrier against flocculation. Further work is needed to determine the relative roll of the electrical double layer stabilization versus steric stabilization.

6. The phosphate ester isotherm exhibits a long, flat, well defined plateau indicative of monolayer coverage. Adsorption concentrations at a monolayer of coverage suggests that the phosphate ester adsorbs with a partial vertical orientation while the isotherm shape indicates strong adsorption with little solvent competition.

7. Tapes were cast having a green density of 55% of theoretical. Green density was dependent on the volume fraction of solids that could be effectively dispersed into the casting slip. The microstructure of the green tapes appeared uniform with minimal voids. The sintered tapes exhibited uniform grain growth and minimal porosity.

8. The rate of loading affects deformation and ultimate tensile strength of green tapes. Tapes exhibited increasingly brittle behavior with increasing loading rates and the ultimate tensile strength increased with increasing loading rates up to 1 cm/min crosshead speed above which the strength no longer increased with increasing loading rates.

9. The method of storage affects the ultimate tensile strength of green tapes. If the tapes are not removed from the glass surface, tensile strengths are appreciably lower than strengths of samples removed from the glass after a short drying period. Otherwise strength increases with aging. Drying rate and humidity also affect tensile strength.

10. Sequence of component addition affects viscosity. When the dispersant is added before the binder-plasticizer system viscosity is lower because the dispersant can adsorb strongly to the powder surface without competition from the binder-plasticizer system.

11. Sequence of component addition affects tensile strengths. When the binder-plasticizer system is added prior to the dispersant, strengths are generally higher due to improved attachment of binders to powder surface.

Summary

The dispersion properties of a high purity barium titanate powder suspended in an azeotrope solution of ethanol and methyl ethyl ketone were studied. A variety of commercial dispersants was evaluated for effectiveness. A phosphate ester, a very effective dispersant, was further studied.

Rheological measurements were made under ambient and dry conditions and as a function of aging time. Dry powders and solvents were found to disperse to a greater degree than powders and solvents containing moisture, and the degree of dispersion was found to increase with time. Minimum viscosity and minimum equilibrium settling volume as a function of phosphate ester concentration occurred at approximately 0.7 vol. %. Powder compacts with a packing factor of 0.63 were obtained at this concentration and tapes were cast to a green density of 55% of theoretical.

An adsorption model for the adsorption of the polyelectrolytic phosphate ester is proposed on the basis of electron donor-acceptor reactions. Dispersion stability is derived from both steric hinderence and electrical double layer repulsion mechanisms.

The results of adsorption experiments are presented as composite adsorption isotherms for the phosphate ester system. The isotherm exhibits a well-defined plateau at a surface concentration corresponding to a monolayer of coverage. Maximum dispersion as measured by rheological and settling methods occurred at a concentration of phosphate ester that corresponds to an initial monolayer of coverage.

The tensile strength of the green tapes was measured under various drying conditions and it was found that drying the tape on the glass plate was damaging to its strength.

The order of addition of the dispersant to the tape casting slip was found to affect both the strength and rheology. Adding the dispersant before the binder and other components resulted in a lower viscosity but also a lower ultimate strength in the green tape than when the dispersant was added last.

REFERENCES

1. C. Hodgkins, TAM Ceramics Inc., Niagara Falls, N.Y., private communication, September, 1982.

2. J. Mitchell and D. Smith, Aquametry, Part III, Vol. 5, 2nd ed., John Wiley and Sons, Inc., N.Y., 1980.

3. W. R. Cannon, Deflocculants for Tape Casting $BaTiO_3$ Dielectrics, Annual Report March 1983 under ONR contact N00014-82-K-0310.

4. E. S. Tormey, "The Adsorption of Glyceryl Esters at the Alumina/Toluene Interface", Ph.D. Thesis, Massachusetts Institute of Technology, December 1982.

5. Y. S. Lipatov and L. M. Sergeeva, Adsorption of POlymers, John Wiley and Sons, Inc., N.Y., 1974.

6. Th. F. Tadros, "Physical Stability of Suspension Concentrates", Advances in Colloid and Interface Science, 12 (1980) 141-261.

7. R. Buscall, Colloids and Surfaces, 5 (1982) 269.

8. D. Quemada, "Rheology of Concentrated Disperse Systems and Minimum Energy Dissipation Principle: I-" Rheologica Acta, 16, 82-94 (1977).

9. C. Chanyavanich, "Rheology of Spherical Silica Particles", Ph.D. Thesis, Rutgers, The State University, May 1983.

10. D. J. Shaw, Introduction to Colloid and Surface Chemistry, 3rd ed., Butterworth and Co. Ltd., 1980.

11. M. Heathe, Witco Chemical Co., New York, N.Y., private conversation, January 1983.

12. P. Somasundaran and D. W. Feuerstenaw, " Mechanisms of Alkyl Sulfonate Adsorption at the Alumina - Water Interface," J. Phys Chem., 70, (1966) 90-96.

13. J. J. Kipling, Adsorption from Solution of Non-Electrolytes, Academic Press Inc., N.Y., 1965.

14. G. D. Parfitt, J. Peacock, "Stability of Colloidal Dispersions in Nonaqueous Media," Surface and Colloid Sci,. Vol. 10, E. Matejevic, Ed., Plenum Press, 1978.

15. F. M. Fowkes, "Mechanisms of Electric Charging Particles in Nonaqueous Liquids," Reprinted from ASC Symposium Series, No. 200, 1982.

16. D. J. Shanefield and R. E. Mistler, "The Characterization of Unfired Tape Cast Ceramics," Reprint Western Electric Co., 1971.

17. D. Tolino, Unpublished Research, Rutgers University, Dept. of Ceramics, October 1983.

18. F. M. Fowkes, J. Ind. Eng. Chem., 17 (1978) 1.

DEPARTMENT OF THE NAVY
OFFICE OF NAVAL RESEARCH
ARLINGTON, VIRGINIA 22217

IN REPLY REFER TO

BASIC DISTRIBUTION LIST

Technical and Summary Reports December 1982

Organization	Codes
Defense Documentation Center Cameron Station Alexandria, VA 22314	12
Office of Naval Research Department of the Navy 800 N. Quincy Street Arlington, VA 22217 Attn: Code 431	3
Naval Research Laboratory Washington, DC 20375 ATTN: Codes 6000 6300 2627	1 1 1
Naval Air Development Center Code 606 Warminster, PA 18974 ATTN: Dr. J. DeLuccia	1
Commanding Officer Naval Surface Weapons Center White Oak Laboratory Silver Spring, MD 20910 ATTN: Library	1
Naval Oceans Systems Center San Diego, CA 92132 ATTN: Library	1
Naval Postgraduate School Monterey, CA 93940 ATTN: Mechanical Engineering Department	1
Naval Air Systems Command Washington, DC 20360 ATTN: Code 31A Code 5304B	1 1
Naval Sea System Command Washington, DC 20362 ATTN: Code 05R	1

Organization	Copies
Naval Air Propulsion Test Center Trenton, NJ 08628 ATTN: Library	1
Naval Construction Battallion Civil Engineering Laboratory Port Hueneme, CA 93043 ATTN: Materials Division	1
Naval Electronics Laboratory San Diego, CA 92152 ATTN: Electron Materials Sciences Division	1
Naval Missile Center Materials Consultant Code 3312-1 Point Mugu, CA 92041	1
Commander David W. Taylor Naval Ship Research and Development Center Bethesda, MD 20084	1
Naval Underwater System Center Newport, RI 02840 ATTN: Library	1
Naval Weapons Center China Lake, CA 93555 ATTN: Library	1
NASA Lewis Research Center 21000 Brookpark Road Cleveland, OH 44135 ATTN: Library	1
National Bureau of Standards Washington, DC 20234 ATTN: Metals Science and Standards Division Ceramics Glass and Solid State Science Division Fracture and Deformation Div.	1 1 1

Naval Facilities Engineering Command
Alexandria, VA 22331
ATTN: Code 03 1

Scientific Advisor
Commandant of the Marine Corps
Washington, DC 20380
ATTN: Code AX 1

Army Research Office
P. O. Box 12211
Triangle Park, NC 27709
ATTN: Metallurgy & Ceramics Program 1

Army Materials and Mechanics Research Center
Watertown, MA 02172
ATTN: Research Programs Office 1

Air Force Office of Scientific Research/NE
Building 410
Bolling Air Force Base
Washington, DC 20332
ATTN: Electronics & Materials Science Directorate 1

NASA Headquarters
Washington, DC 20546
ATTN: Code RRM 1

General Electric Company
P.O. Box 7722
Philadelphia, PA 19101 1

Defense Metals and Ceramics Information Center
Battelle Memorial Institute
505 King Avenue
Columbus, OH 43201 1

Metals and Ceramics Division
Oak Ridge National Laboratory
P.O. Box X
Oak Ridge, TN 37380 1

Los Alamos Scientific Laboratory
P.O. Box 1663
Los Alamos, NM 87544
ATTN: Report Librarian 1

Argonne National Laboratory
Metallurgy Division
P.O. Box 229
Lemont, IL 60439 1

Brookhaven National Laboratory
Technical Information Division
Upton, Long Island
New York 11973
ATTN: Research Library 1

Library
Building 50, Room 134
Lawrence Radiation Laboratory
Berkeley, CA 1

Send ONE COPY to each unless otherwise indicated.

::
RE/431/84/46

January 1984

NEW MULTILAYER CAPACITOR PROGRAM LIST

Professor Harlan U. Anderson
University of Missouri-Rolla
107 Fulton Hall
Rolla, MO 65401

Professor R. Vest
Purdue University
West Lafayette, IN 47907

Dr. John B. Blum
Rutgers University
College of Engineering
P.O. Box 909
Piscataway, NJ 08859

Dr. J. V. Biggers
Pennsylvania State University
Materials Research Laboratory
University Park, PA 16802

Professor R. Buchanan
University of Illinois
Department of Ceramic Engineering
Urbana, IL 61801

Professor Larry Burton
Virginia Polytechnic Institute
and State University
Blacksburg, VA 24061

Professor Roger Cannon
Rutgers University
College of Engineering
P.O. Box 909
Piscataway, NJ 08859

Prof. Donald M. Smyth
Lehigh University
Materials Research Laboratory
Coxe Laboratory 32
Bethlehem, PA 18015

Dr. N. Eror
Oregon Graduate Center
19600 N. W. Walker Road
Beaverton, OR 97006

Dr. K. D. McHenry
Honeywell Ceramics Center
5121 Winnetka ave., N.
New Hope, MN 55428

Professor D. W. Readey
Department of Ceramic Engineering
1314 Kinnear Road
Columbus, OH 43212

Dr. Lew Hoffman
Hoffman Associates
301 Broadway (US 1) Suite 206A
P.O. 10492
Riviera Beach, FL 33404

Dr. Gordon R. Love
Corporate Research, Development
and Engineering
Sprague Electric Co.
North Adams, Mass 01247

Roger T. Dirstine
Ceramics Research
Unitrode Corporation
580 Pleasant St.
Watertown, Mass 02172

Dr. Sidney J. Stein
Electro-Science Laboratories
2211 Sherman Ave
Pennsauken, NJ 08110

John C. Constantine
Electronic Materials Systems
Englehard Industries Division
1 West Central Ave.
E. Newark, NJ 07029

(Continue of Multilayer Capacitor Program List)

John Piper
Union Carbide Corporation
Electronics Division-Components Dept.
P.O. Box 5928
Greenville, SC 29606

Dr. Kim Ritchie
Vice President
Corporate Research Laboratory
AVX Corporation
P.O. Box 867
Myrtle Beach, SC 29577

Tack J. Whang
Technical Center
Ferro Corporation
7500 E. Pleasant Valley Road
Independence, OH 44131

Advanced Research Projects
Materials Science Director
1400 Wilson Boulevard
Arlington, VA 22209

Dr. Gene Haertling
Motorola Corporation
3434 Vassar, NE
Albuquerque, NM 87107

W.B. Harrison
Honeywell Ceramics Center
5121 Winnetka Ave. N.
New Hope, MN 55428

Prof. L. E. Cross
The Pennsylvania State University
Materials Research Laboratory
University Park, PA 16802

Dr. P.L. Smith
Naval Research Laboratory
Code 6361
Washington, DC 20375

Professor R. Roy
The Pennsylvania State University
Materials Research Laboratory
University Park, PA 16802

Dr. R. Rice
Naval Research Laboratory
Code 6360
Washington, DC 20375

Dr. G. Ewell
MS6-D163
Hughes Aircraft Company
Centinela & Teale Streets
Culver City, CA 90230

Dr. George W. Taylor
Princeton Resources, Inc.
P.O. Box 211
Princeton, NJ 08540

Dr. J. Smith
GTE Sylvania
100 Endicott Street
Danvers, MA 01923

Professor R. Buchanan
Department of Ceramic Engineering
University of Illinois
Urbana, Ill 61801

Dr. Wallace A. Smith
North American Philips Laboratories
345 Scarborough Road
Briarcliff Manor, NY 10510

Professor B. A. Auld
Stanford University
W.W. Hansen Laboratories of Physics
Stanford, CA 94306

Mr. G. Goodman, Manager
Corporation of Applied Research
Group
Globe-Union Inc.
5757 North Green Bay Avenue
Milwaukee, WI 53201

Director
Applied Research Lab
The Pennsylvania State Univ.
University Park, PA 16802

(Continue of Multilayer Capacitor Program List)

Army Research Office
Box CM, Duke Station
Attn: Met. & Ceram. Div.
Durham, NC 27706

National Bureau of Standards
Inorganic Mats. Division
Washington, DC 20234

Dr. R. R. Neurgaonkar
Rockwell International Science Center
1049 Camino Dos Rios
P.O. Box 1085
Thousand Oaks, CA 91360

Darnall P. Burks
Sprague Electric Company
P. O. Box 5327
Wichita Falls, TX 76307

Mr. J.D. Walton
Engineering Experiment Station
Georgia Institute of Technology
Atlanta, GA 30332

Roger T. Dirstine
Unitrode Corporation
580 Pleasant Street
Watertown, MASS 02172

Dr. Kim Ritchie
AVX Corporation
P. O. Box 867
Myrtle Beach, SC 29577

Additional Copies

Dr. Von Richards
Argonne National Lab
Materials Sci. Techn. Div.
Bldg. 212
9700 So. Cass Ave.
Argonne, ILL 60439

Dr. T. C. Dean
TAM Ceramics, Inc.
Box C
Bridge Station
Niagara Falls, NY 14305

Mr. Paul Baker
Bourns Inc.
693 West 1700 So. Street
Logan, UTAH 84321

Dr. David Cronin
Trans-Tech
5520 Adamstown Rd.
Adamstown, MD 21710

END

FILMED

10-84

DTIC